REVIEWS OF GEOPHYSICS VOL. 3, NO. 2 MAY 1965

Trapped Orbits in a Magnetic Dipole Field

A. J. DRAGT

Institute for Advanced Study, Princeton, New Jersey

Abstract. This article is a review of the trapped motion of a charged particle in a dipole magnetic field. It provides an extensive discussion of the equations of motion in various coordinate systems and of their solution by approximate and analytically exact methods. Wherever possible, approximate solutions are compared with exact solutions obtained by numerical integration.

1. INTRODUCTION

The problem of determining the motion of a charged particle in the earth's magnetic field enjoys a long history. The problem was first formulated by *Störmer* [1907] and was subsequently studied by him and several others in connection with auroral phenomena and cosmic rays. Because of this connection, particular attention was given to the orbits that enter the earth's field from infinity. More recently, owing to the discovery of the Van Allen radiation [*Van Allen et al.*, 1958], a knowledge of orbits that are trapped within the earth's field has also become important. The aim of this paper is to review the essential features of these trapped orbits in the approximation that the earth's field is replaced by that of a static magnetic dipole. (For a discussion of the more general case, see the work of *Hones* [1963], *Northrop* [1963*a*, *b*], and *Ray* [1963].)

It is convenient to begin with a qualitative description of the particle motion. Consider a low-energy particle of charge q and mass m placed in a magnetic dipole field of moment $\mathfrak{M}$ as shown in Figure 1. Then, by intuition one expects that the

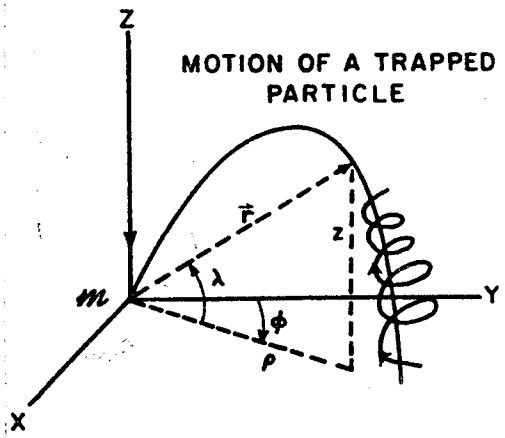

Fig. 1. Schematic representation of trapped charged particle motion in a magnetic dipole field. Note that with the conventional choice of geographic coordinates, the earth's magnetic moment $\mathfrak{M}$ points down.

particle will gyrate about a guiding line of force

$$r = r_0 \cos^2 \lambda \tag{1.1}$$

with the cyclotron frequency

$$\omega = qB/\gamma m \tag{1.2}$$

where

$$\gamma = [1 - (v^2/c^2)]^{-1/2} \tag{1.3}$$

$$\mathbf{B} = \nabla \times \mathbf{A} \tag{1.4}$$

$$\mathbf{A} = \hat{\phi}\mathfrak{M}\rho r^{-3} \tag{1.5}$$

$$B = \frac{\mathfrak{M}}{r^3}(1 + 3\sin^2\lambda)^{1/2} \tag{1.6}$$

In addition, the particle will move along the line of force, making its actual orbit resemble a spiral. As it moves into regions of stronger field at higher latitudes, it will be reflected back toward the equator by converging lines of force. The result is a bouncing motion back and forth across the equatorial plane. Finally, the line of force about which the particle spirals will slowly drift in longitude.

In the following sections these intuitive conclusions are made more precise. Section 2 contains a discussion of the equations of motion in several different coordinate systems and their few known exact solutions. Section 3 deals with approximate solutions to the equations of motion developed by Alfvén. In section 4, an alternate method for determining approximate solutions based on the use of an action integral is developed. It is employed in section 5 to determine various features of the motion for which simple Alfvén theory is inadequate. A final section enters into a speculative discussion of the validity of perturbative solutions for long times. Wherever possible, approximate solutions are supplemented by examples of exact solutions obtained numerically. The method of numerical integration is given in an appendix.

2. EQUATIONS OF MOTION

The equations of motion for the Störmer problem form a nonlinear set of coupled, second-order, differential equations. It is therefore not surprising that they do not possess any simple analytical solution. In this section we shall simplify them as much as possible and discuss what information is known about their solution.

There are several ways of writing the differential equations for the Störmer problem. For our purposes it is most convenient to employ a canonical formulation described by the relativistic Hamiltonian:

$$\mathcal{H}_R = \{m^2c^4 + c^2[p_z^2 + p_\rho^2 + ((p_\phi/\rho) - qA_\phi)^2]\}^{1/2} \tag{2.1}$$

where

$$p_z = \gamma m\dot{z} \tag{2.2}$$

$$p_\rho = \gamma m\dot{\rho} \tag{2.3}$$

$$p_\phi = \gamma m\rho^2\dot{\phi} + q\rho A_\phi \tag{2.4}$$

Since the Hamiltonian is independent of the time, the energy is a constant of motion

$$\mathcal{H}_R = \gamma mc^2 = \text{constant} \tag{2.5}$$

The constancy of $\mathcal{H}_R$ and γ makes it possible to introduce a new Hamiltonian, $\mathcal{H}$, which is equivalent to $\mathcal{H}_R$ and has a simpler form that resembles a nonrelativistic Hamiltonian

$$\mathcal{H} = (1/2\gamma m)[p_z^2 + p_\rho^2 + ((p_\phi/\rho) - qA_\phi)^2] \tag{2.6}$$

If one regards γ as a constant, one finds that $\mathcal{H}_R$ and $\mathcal{H}$ have identical partial derivatives with respect to all dynamical variables and are therefore equivalent. $\mathcal{H}$ is also conserved

$$\mathcal{H} = \tfrac{1}{2}\gamma mv^2 = \text{constant} \tag{2.7}$$

In what follows, we shall always use $\mathcal{H}$ in place of $\mathcal{H}_R$.

A second constant of motion follows from the invariance of $\mathcal{H}$ under rotations about the z axis

$$\dot{p}_\phi = -\partial\mathcal{H}/\partial\phi = 0 \tag{2.8}$$

or

$$p_\phi = q\mathfrak{M}\Gamma \tag{2.9}$$

where the integration constant Γ has the dimensions of a reciprocal length.

The three-dimensional problem is thus reduced to the simpler problem of finding the two-dimensional motion of a particle in the $\rho - z$ plane under the influence of the potential

$$V = (1/2\gamma m)[(q\mathfrak{M}\Gamma/\rho) - qA_\phi]^2 \tag{2.10}$$

Once this problem has been solved to find $\rho(t)$ and $z(t)$, $\phi(t)$ may be found by integrating equation 2.4

$$\phi(t) = \int \frac{dt}{\gamma m\rho^2}(q\mathfrak{M}\Gamma - q\rho A_\phi) \tag{2.11}$$

So far, the sign of Γ has not been determined. Examination of V shows that its radial derivative is always negative unless Γ is positive:

$$\mathbf{r}\cdot\nabla V = -\frac{q^2\mathfrak{M}^2}{\gamma m}\left[\frac{\Gamma}{\rho} - \frac{\rho}{r^3}\right]\left[\frac{\Gamma}{\rho} - \frac{2\rho}{r^3}\right] \tag{2.12}$$

A negative radial derivative for the potential corresponds to a repulsive radial force. Consequently, all orbits characterized by a negative Γ must extend to infinity and cannot be trapped. When Γ is positive, V has a minimum on the line

$$r = \Gamma^{-1}\cos^2\lambda \tag{2.13}$$

Particles of sufficiently low energy will be confined to the vicinity of this line, and we have

$$r_0 = \Gamma^{-1} \tag{2.14}$$

To examine what is meant by 'sufficiently low energy,' it is useful to simplify the problem further by the introduction of dimensionless variables

$$z' = \Gamma z \tag{2.15a}$$

$$\rho' = \Gamma \rho \tag{2.15b}$$

$$\phi' = \phi \tag{2.15c}$$

$$t' = \Gamma^3 q \mathfrak{M} (\gamma m)^{-1} t \tag{2.15d}$$

Equations 2.6, 2.7, 2.10, and 2.11 now take the simpler form

$$\mathfrak{K} = \tfrac{1}{2}(p_z^2 + p_\rho^2) + V \tag{2.16}$$

$$V = \tfrac{1}{2}[(1/\rho) - (\rho/r^3)]^2 \tag{2.17}$$

$$\mathfrak{K} = \text{constant} = 1/32\gamma_1^4 \tag{2.18}$$

$$\phi = \int dt\, [(1/\rho^2) - (1/r^3)] \tag{2.19}$$

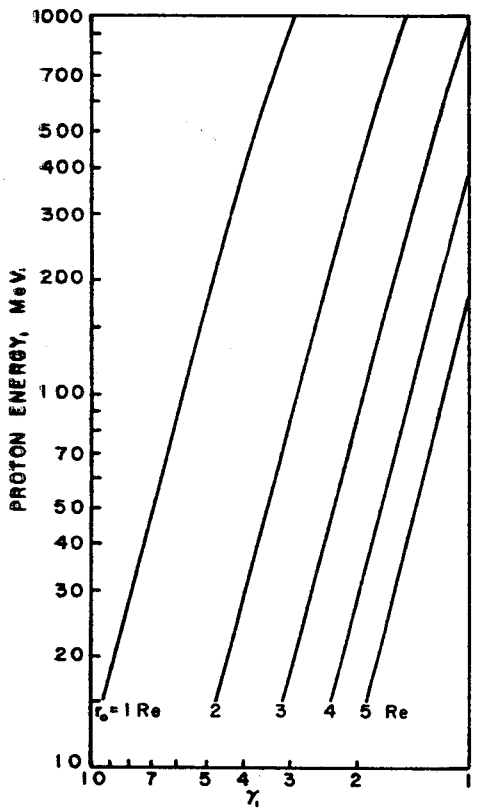

Fig. 2

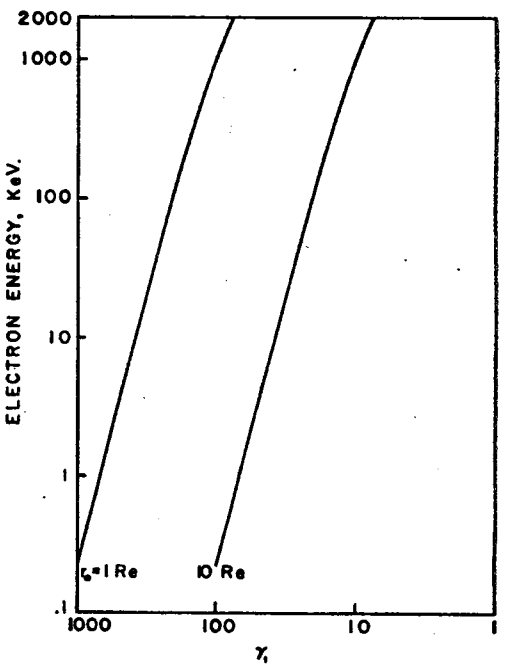

Fig. 3

Figs. 2–3. Values of γ_1 for particles and energies relevant to the Van Allen radiation. The particles are labeled according to their guiding field line with r_0 given in earth radii. ($\mathfrak{M}$ = 8.06×10^{25} gauss cm^3. R_e = radius of the earth = 6,378 km.

where the primes have been suppressed for notational convenience. The dimensionless constant γ_1 of equation 2.18 is that used by *Störmer* [1955, pp. 219–224][1] and is related to the constants of equations 2.7 and 2.9 by

$$\gamma_1^4 = \frac{1}{16}\left(\frac{q\mathfrak{M}}{v\gamma m}\right)^2 \Gamma^4 \tag{2.20}$$

In this system of units, the particle gyrates about the guiding field line

$$r = \cos^2 \lambda \tag{2.21}$$

with unit frequency when in the equatorial plane and has the dimensionless velocity

$$W_0 = 1/4\gamma_1^2 \tag{2.22}$$

The values of γ_1 for particles and energies relevant to the Van Allen radiation are given in Figures 2 and 3. For ease of computation, the relation between W_0^2 and γ_1 is plotted in Figure 4.

We now examine V in greater detail by constructing a contour map as shown in Figure 5. Inspection of the map shows that V vanishes on the floor of the valley (thalweg) given by equation 2.21 and at $\rho = \infty$, and it is positive elsewhere.

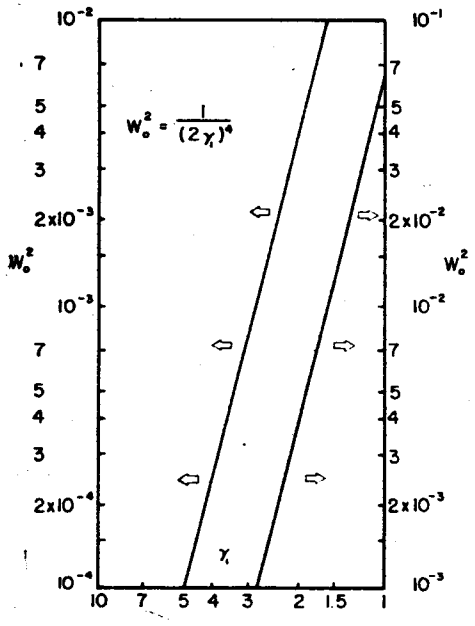

Fig. 4. The relationship between W_0^2 and γ_1.

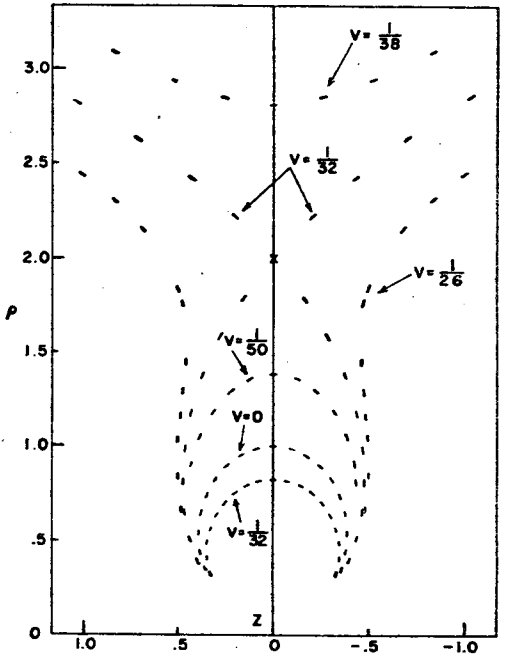

Fig. 5. A contour map of V showing lines of constant potential.

[1] This book is a primary reference to work done on motion in a dipole field up to 1955. It contains an extensive discussion of the equations of motion and their solution by numerical integration.

Moreover, there is a pass connecting the thalweg to infinity at $z = 0, \rho = 2$, where V has the value

$$V = 1/32 \tag{2.23}$$

All other paths leading from the thalweg to infinity and not going through the pass encounter larger values of V. One concludes from energy conservation that particles in the valley will be trapped provided their total energy is less than 1/32 or $\gamma_1 > 1$. These particles must remain in the vicinity of the field line given by equation 2.21 or, in the old variables, the field line given by equation 1.1. Here is the justification for our intuitive notion that low-energy particles are confined to magnetic field lines.

Unfortunately, there are no further known constants of motion, so that the system of equations 2.16–2.18 is as simple a system as one can achieve. In general, it has no known analytic solution. The equations can, however, be solved in terms of elliptic functions for the special initial conditions

$$z = \dot{z} = 0 \tag{2.24}$$

in which case the orbit is confined to the equatorial plane [*Graef and Kusaka*, 1938; *De Vogelaere*, 1950].

The behavior of the equatorial orbits for small excursions out of the equatorial plane may be examined by perturbation methods. Expanding V as a power series in z and applying Hamilton's equations, one obtains

$$\ddot{z} + (1/\rho^6)(\rho - 1)z = 0 + O(z^3) \tag{2.25}$$

$$\ddot{\rho} + (1/\rho^5)(\rho - 1)(2 - \rho) = 0 + O(z^2) \tag{2.26}$$

If the terms of second and higher order in z are neglected, the solution to equation 2.26 is the same as the equatorial case and is therefore a known periodic function of time. Equation 2.25 then becomes Hill's equation [*Whittaker and Watson*, 1958]. Its solution can be written in the form

$$z = Ce^{\Omega t}\psi(t) + De^{-\Omega t}\psi(-t) \tag{2.27}$$

where C and D are arbitrary constants and $\psi(t)$ is periodic in time with the same period as $\rho(t)$. The constant Ω, called the characteristic Poincaré exponent, determines the stability of the orbit. If Ω has a real part, the motion in the z direction can grow (within the approximations made) without bound. If Ω is purely imaginary, the motion is bounded (for time intervals in which the neglected terms have negligible effect) and is therefore stable. The behavior of Ω as a function of γ_1 has been studied by *De Vogelaere* [1950], who finds that all orbits are stable for $\gamma_1 > 1.3137$.

Besides the analytical solution for motion in the equatorial plane, there is one other available solution which takes the form of a power series in W_0^2. (The solution presented here has previously been given in the form of a double power series in W_0^2 and w. See *Störmer* [1955, pp. 247–248].) We begin by rewriting the equations of motion for the dimensionless ρ and z variables in terms of two new variables given by the equations

$$r = \sqrt{z^2 + \rho^2} \tag{2.28}$$

$$w = \cos^2 \lambda \tag{2.29}$$

The result is

$$r^4(\tfrac{1}{2}(d^2/dt^2)(r^2) - W_0^2) + r - w = 0 \tag{2.30}$$

$$4w(1 - w)r^4[(dr/dt)^2 - W_0^2] + r^6(dw/dt)^2 + 4(1 - w)(w - r)^2 = 0 \tag{2.31}$$

Now let r be regarded as a function of w. Equation 2.31 may be rewritten as

$$(\dot{w})^2[4w(1 - w)r^4r'^2 + r^6] = [W_0^2 4w(1 - w)r^4 - 4(w - r)^2(1 - w)] \tag{2.32}$$

where the prime denotes differentiation with respect to w. We suppose that $r(w, W_0^2)$ can be expanded in the form

$$r = w + \sum_{n=1}^{\infty} W_0^{2n} A_n(w) \tag{2.33}$$

(Since $w \leq 1$ by equation 2.29, the left hand side of Equation 2.32 is always positive. Therefore $r \to w$ as $W_0^2 \to 0$ in order for the equation to hold true.) This assumption permits a similar expansion for $(\dot{w})^2$:

$$(\dot{w})^2 = \sum_{1}^{\infty} W_0^{2n} B_n(w) \tag{2.34}$$

where the coefficients are determined by equations 2.32 and 2.33. The first two are given by

$$B_1 = 4w^5(1 - w)[4w^5(1 - w) + w^6]^{-1} \tag{2.35}$$

$$B_2 = 4w^5(1 - w)[4w^5(1 - w) + w^6]^{-2} \cdot [(3w - 4)A_1^2 - 2w^5 A_1 - 8w^5(1 - w)A_1'] \tag{2.36}$$

We shall also need the expansion for $\ddot{w}$ which follows upon differentiating equation 2.34:

$$\ddot{w} = \tfrac{1}{2} \sum_{1}^{\infty} W_0^{2n} B_n'(w) \tag{2.37}$$

Next consider the quantity $(\ddot{r}^2)$ which occurs in equation 2.30. From equation 2.33 it follows that this quantity can be written as

$$\frac{1}{2}\frac{d^2r^2}{dt^2} = (\dot{w})^2 + w\ddot{w} + W_0^2[\ddot{w}(A_1 + wA_1') + (\dot{w})^2(2A_1' + wA_1'')] + \cdots \tag{2.38}$$

Substitution of the expressions for $(\dot{w})^2$ and $\ddot{w}$ given by equations 2.34 and 2.37 into equation 2.38 gives the result that

$$\frac{1}{2}\frac{d^2r^2}{dt^2} = \sum_{1}^{\infty} W_0^{2n} C_n(w) \tag{2.39}$$

where

$$C_1 = B_1 + \frac{wB_1'}{2} \tag{2.40}$$

$$C_2 = B_2 + \frac{wB_2'}{2} + \frac{B_1'}{2}(A_1 + wA_1') + B_1(2A_1' + wA_1'') \tag{2.41}$$

We now have expansions for all the terms appearing in equation 2.30, which may be rewritten as

$$\left[w + \sum_1^\infty W_0^{2n}A_n\right]^4\left[-W_0^2 + \sum_1^\infty W_0^{2n}C_n\right] + \sum_1^\infty W_0^{2n}A_n = 0 \tag{2.42}$$

Equating powers of W_0^2 gives the recursion relations

$$A_1 = w^4(1 - C_1) \tag{2.43}$$

$$A_2 = (4/w)A_1^2 - C_2w^4, \quad \text{etc.} \tag{2.44}$$

Examination of equations 2.35, 2.36, 2.40, and 2.41 shows that the recursion relations are self-starting and have a unique solution. The first two of the A_n are given by

$$A_1 = 3w^5(2 - w)/(4 - 3w)^2 \tag{2.45}$$

$$A_2 = -[18w^9/(4 - 3w)^6](57w^4 - 357w^3 + 864w^2 - 968w + 400) \tag{2.46}$$

Thus, to terms of order W_0^6,

$$r = w + 3W_0^2w^5(2 - w)/(4 - 3w)^2 + W_0^4A_2 \tag{2.47}$$

To complete our discussion, we must examine the convergence of our assumed series expansion for $r(w, W_0^2)$, equation 2.33. We first observe that the $A_n(w)$ are both well defined by the recursion relations and analytic for all w in the interval $0 \leq w \leq 1$. Consequently the series represents for each value of W_0 an orbit that extends all the way down the guiding field line to the origin of the dipole. The existence of such an orbit has been demonstrated by *Malmquist* [1944]. The uniqueness of this orbit has not yet been proved, but it seems intuitively clear. (The difficulty arises from the singular nature of the equations of motion near $r = 0$ as evidenced by equations 1.2 and 1.6.) Now it is known from numerical studies that this orbit to the origin does not cross the equatorial plane at right angles [*Störmer*, 1913]. That is, $dr/d\lambda|_{\lambda=0} \neq 0$. On the other hand, if we differentiate equation 2.33 under the summation sign we find

$$\left.\frac{dr}{d\lambda}\right|_{\lambda=0} = \left.\frac{dw}{d\lambda}\right|_{\lambda=0} + \sum_1^\infty W_0^{2n}A_n'(w)\left.\frac{dw}{d\lambda}\right|_{\lambda=0} = 0 \tag{2.48}$$

Therefore our series is not the power series expansion of a function which is analytic in W_0 about $W_0 = 0$. Rather, it is an asymptotic series. It is still useful in the sense that

$$\lim_{W_0 \to 0} \frac{r(w, W_0^2) - w - \sum_1^N W_0^{2n}A_n(w)}{W_0^{2N}} = 0 \tag{2.49}$$

We may also conclude that $dr/d\lambda|_{\lambda=0}$ for the orbits to the origin goes to zero with decreasing W_0 faster than any power of W_0. These results are illustrated at the equatorial crossing for orbits obtained numerically in Figures 6 and 7.

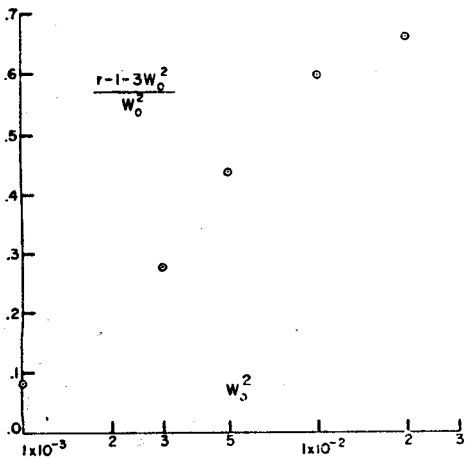

Fig. 6. A numerical illustration of the relation 2.49 with $N = 1$ and $w = 1$ for orbits going to the origin.

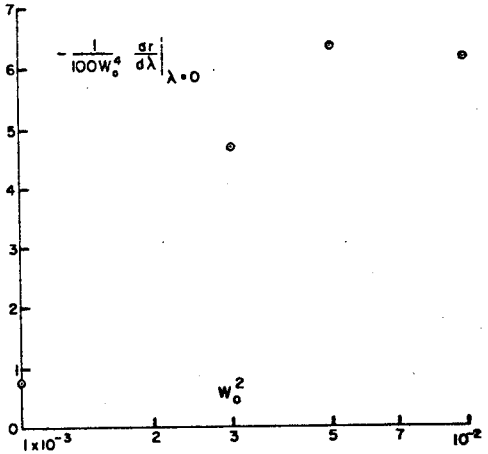

Fig. 7. The approach of $dr/d\lambda|_{\lambda=0}$ to zero with decreasing W_0. For ease of plotting, the derivative has been divided by 100 W_0^4.

As remarked earlier, the equations of motion derived from the Hamiltonian of equation 2.16 are very singular near the origin. This is essentially because the cyclotron frequency governing the gyrations about the guiding field line (or, equivalently, the oscillations about the thalweg) is given, in dimensionless coordinates, by

$$\omega = (1 + 3\sin^2\lambda)^{\frac{1}{2}}/r^3 \tag{2.50}$$

As a result, it is very difficult numerically to integrate trajectories approaching the vicinity of the origin. To obtain an accurate numerical solution, it is necessary to use a time step that is a small fraction of the cyclotron period. The cyclotron period goes to zero as ω^{-1} upon approach to the origin. Consequently it is necessary to make frequent changes in the time step during the course of integration, generally a very inconvenient process.

We shall now explore to what extent this difficulty can be remedied by a change of variables including the time. In making changes in the time scale, it is convenient to employ a 'zero energy' Lagrangian formulation of the equations of motion. We shall use the Lagrangian

$$\mathfrak{L} = \{\dot\rho^2 + \dot z^2 + W_0^2 - [1/\rho - \rho/r^3]^2\} \tag{2.51}$$

which clearly leads to the same equations of motion as the Hamiltonian 2.16. It is called 'zero energy' because for the solution satisfying

$$\dot\rho^2 + \dot z^2 + (1/\rho - \rho/r^3)^2 = W_0^2 \tag{2.52}$$

$$E = \dot z(\partial L/\partial \dot z) + \dot\rho(\partial\mathfrak{L}/\partial\dot\rho) - \mathfrak{L} = 0 \tag{2.53}$$

We now use the fact [*Birkhoff*, 1927, p. 38] that under a change of time variables $t \to l$, $\mathfrak{L} \to \bar{\mathfrak{L}}$ with

$$\mathfrak{L}\, dt = \bar{\mathfrak{L}}\, dl \tag{2.54}$$

$\bar{\mathfrak{L}}$ also has zero energy. Writing

$$d\bar{t} = f(\rho,z)\, dt \tag{2.55}$$

gives

$$\bar{\mathfrak{L}} = f(\rho'^2 + z'^2) + (1/f)[W_0^2 - V(\rho, z)] \tag{2.56}$$

where primes denote differentiation with respect to $\bar{t}$.

The new Lagrangian would again take a simple form if we could find new coordinates $\xi(\rho, z)$ and $\eta(\rho, z)$ such that

$$d\xi^2 + d\eta^2 = f(d\rho^2 + dz^2) \tag{2.57}$$

For this to be possible, the metric for the line element

$$ds^2 = f(d\rho^2 + dz^2) \tag{2.58}$$

must have a zero curvature tensor [*Eisenhart*, 1947]. What we would like to do is set $d\bar{t} = \omega\, dt$ because this would make the transformed cyclotron frequency a constant. Unfortunately this is impossible since the line element (2.58) with $f = \omega$ does not have zero curvature. It is possible, however, to get rid of the worst part, the r^{-3} term, and set

$$f = r^{-3} \tag{2.59}$$

Let

$$w = \rho + iz \tag{2.60}$$

and

$$\zeta = \xi + i\eta \tag{2.61}$$

be two complex variables. Then

$$w = re^{i\lambda} \tag{2.62}$$

and

$$d\rho^2 + dz^2 = dw\, dw^*, \quad \text{etc.} \tag{2.63}$$

Thus

$$d\zeta\, d\zeta^* = (ww^*)^{-3/2}\, dw\, dw^* \tag{2.64}$$

with the possible solution

$$\zeta = 2e^{i\psi}w^{-1/2} \tag{2.65}$$

where ψ is an arbitrary phase factor. Equating real and imaginary parts and setting $\psi = \pi/4$ gives

$$\xi = (2/r)^{1/2}(\cos\lambda/2 + \sin\lambda/2) \tag{2.66a}$$

$$\eta = (2/r)^{1/2}(\cos\lambda/2 - \sin\lambda/2) \tag{2.66b}$$

and the inverse relations

$$r = 4(\xi^2 + \eta^2)^{-1} \tag{2.67a}$$

$$\cos \lambda = 2\xi\eta(\xi^2 + \eta^2)^{-1} \tag{2.67b}$$

Other choices for the angle ψ merely lead to a rotation of coordinates in the ξ, η plane. Substituting the expressions for the new coordinates into equation 2.56 and remembering the relations

$$= r \sin \lambda \tag{2.68a}$$

$$\rho = r \cos \lambda \tag{2.68b}$$

gives the final Lagrangian

$$\bar{\mathfrak{L}} = \xi'^2 + \eta'^2 - U(\xi, \eta) \tag{2.69}$$

with

$$U = (\xi^2 + \eta^2)^{-1}[(\xi^2 + \eta^2)/(\xi\eta) - \xi\eta]^2 - (64W_0^2)(\xi^2 + \eta^2)^{-3} \tag{2.70}$$

The new equations of motion are

$$\xi'' = -\tfrac{1}{2}(\partial U/\partial \xi) \tag{2.71a}$$

$$\eta'' = -\tfrac{1}{2}(\partial U/\partial \eta) \tag{2.71b}$$

along with the subsidary zero energy condition

$$\xi'^2 + \eta'^2 + U = 0 \tag{2.72}$$

Finally the thalweg, equation 2.21, is transformed into the curve

$$\xi^2 + \eta^2 = \xi^2\eta^2 \tag{2.73}$$

Examination of the behavior of U reveals that both ξ'' and η'' are analytic functions of ξ and η within the region $U \leq 0$ allowed by equation 2.72, including the points at infinity, which are the images of the origin in the old coordinates. Furthermore, the transformed cyclotron frequency varies at most by a factor of 2 over the entire thalweg since only the factor $\sqrt{1 + 3\sin^2 \lambda}$ remains. We conclude that equations 2.71 are much better suited for numerical integration than those with which we began. The price that has been paid is that the origin $r = 0$ has been transformed to infinity. This means that the orbits that used to go to the origin now go to infinity. Consequently, these orbits still have a rather special character. (For a coordinate transformation setting $f = r^{-2}$, see *Störmer* [1955, pp. 225–227]. This choice is less satisfactory since the transformed cyclotron frequency is still singular at the image of the origin. The coordinate system given here should also be useful for cosmic-ray orbits.)

3. ALFVÉN THEORY

Because there are no known analytical solutions for general initial conditions (initial conditions that do not lead to equatorial orbits or the trajectory to the origin), it is necessary to resort to approximate solutions or numerical integration. In this section a brief review is given of the approximate solutions developed by *Alfvén* [*Alfvén*, 1950; *Alfvén and Falthammar*, 1963]. In its greatest generality, Alfvén's method is applicable to time-dependent fields without axial symmetry.

Our discussion will be restricted, however, to the case of a static dipole field. An alternate approach to that of Alfvén will be developed with the use of canonical perturbation theory in the next section.

Since the appearance of Alfvén's pioneering work in the 1940's, considerable effort has been devoted to expanding his results, both by calculations similar in spirit to his own and by methods employing canonical perturbation theory. The current state of the art is well summarized in the book of *Northrop* [1963*a*], to which the reader is referred for further information and an extensive bibliography. In addition, the reader is referred to papers of *Lemaitre and Bossy* [1945], *Bossy* [1962], *Gall* [1963], *Hayakawa and Obayashi* [1963], and references cited therein.

Alfvén begins with the particle motion in a homogeneous field and then introduces the inhomogeneity as a perturbation. In such an approximation the motion may be decomposed into the composite of two motions, gyration about a point called the guiding center and motion of the guiding center itself. These motions may each be discussed separately and then recombined to find the total motion.

Consider first the gyrating motion. For the case that the magnetic field $\mathbf{B}(\mathbf{r})$ encountered by a gyrating particle varies slowly during a cyclotron period, Alfvén shows that the magnetic moment M

$$M = v_\perp^2/2\omega \tag{3.1}$$

associated with this motion is nearly constant. The slow change in the magnetic field may arise either from an explicit time dependence of B or from the change in B experienced by a particle, owing to its motion. The quantity $v_\perp$ is defined as the component of the velocity perpendicular to the magnetic field. This result provides a constant of motion for the gyrating part.

The description of the guiding center motion is more complicated. Alfvén shows that it drifts with a velocity $\mathbf{u}$ having a component perpendicular to the field

$$\mathbf{u}_\perp = (1/qB^2)[\mathbf{B} \times (qM\nabla B + \gamma m\dot{\mathbf{u}})] \tag{3.2}$$

whereas the component along the field is governed by the equation

$$\gamma m\dot{u}_\parallel + qM\nabla_\parallel B = 0 \tag{3.3}$$

In equations 3.1–3.3, B is evaluated at the guiding center.

These results may now be applied to the dipole field. Multiplying equation 3.3 by $\mathbf{u}_\parallel$ and integrating, one obtains

$$\tfrac{1}{2}\gamma m u_\parallel^2 + qMB = \text{constant} \tag{3.4}$$

Comparison of equations 3.1 and 3.4 and energy conservation shows that within the approximations made, $u_\parallel = v_\parallel$ where $v_\parallel$ is the component of the particle velocity parallel to the magnetic field. Consequently equation 3.4 may be rewritten as

$$dl/dt = u_\parallel = [v^2 - (2qBM/\gamma m)]^{1/2} \tag{3.5}$$

where l is the distance measured along the magnetic field line. For the particular case of a particle gyrating about the guiding field line of equation 1.1, B and l are

given by the equations

$$B(\lambda) = B_0(1 + 3\sin^2\lambda)^{1/2}(\cos\lambda)^{-6} \tag{3.6}$$

$$B_0 = \mathfrak{M}r_0^{-3} \tag{3.7}$$

$$dl = r_0\cos\lambda\,(1 + 3\sin^2\lambda)^{1/2}\,d\lambda \tag{3.8}$$

Examination of equations 3.5 and 3.6 reveals that $u_\parallel$ vanishes when B assumes the value B_m

$$B_m = \gamma mv^2/2qM \tag{3.9}$$

Consequently the particle will mirror at this point and be reflected back toward the equator. This is the most significant geophysical result of Alfvén's method, since it shows that the Van Allen radiation is prevented from entering the earth's denser atmosphere where it would be quickly lost. Of course, the result is only correct to the extent that M remains approximately constant. The long-term behavior of M will be discussed in section 6.

In what follows it is convenient to introduce a dimensionless parameter μ defined by

$$\mu^2 = \frac{2qB_0M}{\gamma mv^2} = \frac{v_\perp^2}{v^2}\bigg|_{z=0} \tag{3.10}$$

The quantity μ is the sine of the angle between the particle velocity and the magnetic field at the moment the particle crosses the equatorial plane. Equation 3.5 may now be solved by integration:

$$t(\lambda, \lambda_m) = \frac{1}{v}\int_0^\lambda d\lambda'\,\frac{dl}{d\lambda'}\left(1 - \mu^2\frac{B(\lambda')}{B_0}\right)^{-1/2} \tag{3.11}$$

$$= \frac{r_0}{v}\,T(\lambda, \lambda_m)$$

where the mirror latitude λ_m is given by

$$B(\lambda_m) = B_m = B_0/\mu^2 \tag{3.12}$$

The integral has been evaluated numerically in the special case $\lambda = \lambda_m$ to obtain the bounce period $T(\mu) = T(\lambda_m, \lambda_m)$ [*Hamlin et al.*, 1961]. The results are reproduced in Table 1.

In essence, equations 3.1 and 3.11 give an approximate solution for the ρ-z motion governed by equation 2.6. Now consider the problem of integrating equation 2.11 to find $\phi(t)$. For the dipole field, equation 3.2 may be simplified to read

$$u_\perp = (\omega R)^{-1}[\tfrac{1}{2}v_\perp^2 + v_\parallel^2] \tag{3.13}$$

The result follows from the relations

$$(1/B)\nabla_\perp B = 1/R \tag{3.14}$$

$$\dot{\mathbf{u}}_\perp = v_\parallel^2/R \tag{3.15}$$

$$R = (r_0/3)\cos\lambda(1 + 3\sin^2\lambda)^{3/2}/(1 + \sin^2\lambda) \tag{3.16}$$

TABLE 1. Orbital Characteristics as a Function of μ

λ_m	B_m/B_0	μ	μ^2	$T(u)$	$E(u)$	$I(u)$	$\mu^2 N(u)$	$N(u)$
0	1	1.000	1.000	.7405	.3702	0	.943	.943
4	1.022	9.891^{-1}	9.783^{-1}	.7449	.3711	.016	.938	.959
8	1.091	9.575^{-1}	9.168^{-1}	.7601	.3747	.065	.926	1.010
12	1.213	9.078^{-1}	8.241^{-1}	.7842	.3804	.141	.909	1.103
16	1.404	8.438^{-1}	7.120^{-1}	.8159	.3876	.243	.884	1.241
20	1.688	7.697^{-1}	5.924^{-1}	.8535	.3960	.369	.852	1.438
25	2.236	6.687^{-1}	4.472^{-1}	.9063	.4072	.552	.802	1.793
30	3.136	5.647^{-1}	3.189^{-1}	.9626	.4183	.758	.743	2.330
35	4.664	4.630^{-1}	2.144^{-1}	1.020	.4285	.979	.675	3.148
40	7.402	3.675^{-1}	1.351^{-1}	1.076	.4374	1.210	.600	4.44
45	1.265^{1}	2.812^{-1}	7.907^{-2}	1.129	.4446	1.445	.518	6.55
50	2.356^{1}	2.060^{-1}	4.244^{-2}	1.179	.4501	1.677	.434	1.02^{1}
55	4.876^{1}	1.432^{-1}	2.051^{-2}	1.224	.4541	1.901	.348	1.70^{1}
60	1.154^{2}	9.310^{-2}	8.668^{-3}	1.264	.4568	2.109	.267	3.08^{1}
65	3.267^{2}	5.533^{-2}	3.061^{-3}	1.298	.4584	2.295	.192	6.27^{1}
70	1.193^{3}	2.895^{-2}	8.381^{-4}	1.327	.4594	2.456	.126	1.50^{2}
75	6.481^{3}	1.242^{-2}	1.543^{-4}	1.350	.4598	2.586	.073	4.73^{2}
80	7.210^{4}	3.724^{-3}	1.387^{-5}	1.366	.4600	2.681	.032	2.3^{3}
85	4.550^{6}	4.688^{-4}	2.198^{-7}	1.376	.4600	2.740	.008	3.6^{4}
90	∞	0	0	1.380	.4601	2.751	.006	∞

where R is the radius of curvature for the guiding field line. The average value of $\dot{\phi}$ over a gyration is now given by

$$\bar{\dot{\phi}} = u_\perp/\rho \tag{3.17}$$

The accuracy of this result may be checked for the special case of equatorial orbits [*Avrett*, 1962]. When $v_\parallel$ is zero, equation 3.17 reduces to

$$\bar{\dot{\phi}} = (3/2)(\gamma m/qB_0)(v^2/r_0^2) \tag{3.18a}$$

The exact result obtained by integrating the elliptic functions described in section 2 is given by

$$\bar{\dot{\phi}} = (3/2)(\gamma m/qB_0)(v^2/r_0^2)[1 + (5/4)(v/\omega r_0)^2 + \cdots] \tag{3.18b}$$

When rewritten in terms of the dimensionless variable of section 2, the same equations read

$$\bar{\dot{\phi}} = (3/2)W_0^2 \tag{3.18c}$$

$$\bar{\dot{\phi}} = (3/2)W_0^2[1 + (5/4)W_0^2 + \cdots] \tag{3.18d}$$

A comparison of equations 3.18*c*, *d* with the aid of Figures 2, 3, and 4 shows that the approximate result is adequate for all but the very highest energies.

The general expression for $\bar{\dot{\phi}}$ may be integrated over a bounce period to obtain the total drift per bounce in the form

$$\Delta\phi = 4\int_0^{\lambda_m} \bar{\dot{\phi}} \frac{dl}{d\lambda}\frac{d\lambda}{v_\parallel} = \frac{12\gamma mv}{qB_0 r_0} E(\mu) \tag{3.19}$$

This integral has also been evaluated numerically, and the results are reproduced in Table 1 [*Hamlin et al.*, 1961].

We conclude that within the approximations made, Alfvén's approach gives a complete description of the particle motion. These approximations are expected to become exact in the limit that the particle cyclotron frequency is constant over a cyclotron period, or

$$\dot{\omega}/\omega^2 \ll 1 \tag{3.20}$$

By equations 1.2 and 3.14 this condition is equivalent to requiring that

$$v/\omega R \ll 1 \tag{3.21}$$

In the dimensionless variables, the quantities ω and R are of order unity, whereas the velocity W_0 is given by $(2\ \gamma_1)^{-2}$. The analogous requirement in these variables is therefore that

$$\gamma_1 \gg 1 \tag{3.22}$$

4. CANONICAL PERTURBATION THEORY

In this section we shall formulate an approach to the Störmer problem based on action integrals. This method enjoys the advantage over Alfvén's perturbation theory of giving more accurate results and employing the familiar tools of classical mechanics. It suffers the disadvantage of being readily applicable only to time-independent fields with axial symmetry.

Our discussion will be confined to the two-dimensional motion in the ρ-z plane described by the Hamiltonian of equation 2.16. This is the real problem of interest since, once this motion is known, the motion in three dimensions can be found by a quadrature. In section 2, it was shown that trapped particles are constrained to remain in the vicinity of the thalweg, equation 2.21; hence, the motion may be described as an oscillation about the thalweg superimposed upon motion along the thalweg. This suggests that the problem can best be handled by the introduction of new orthogonal 'dipolar' coordinates, a and b [*Dragt*, 1961]. They are related to the coordinates r and λ by the equations

$$r = a \cos^2 \lambda \tag{4.1a}$$

$$r^2 = b^{-1} \sin \lambda \tag{4.1b}$$

The line element for the a-b coordinates is given by

$$ds^2 = (h_a\, da)^2 + (h_b\, db)^2 \tag{4.2}$$

with

$$h_a{}^2 = (\partial \mathbf{r}/\partial a)^2 = \cos^6 \lambda (1 + 3 \sin^2 \lambda)^{-1} \tag{4.3}$$

$$h_b{}^2 = (\partial \mathbf{r}/\partial b)^2 = a^6 \cos^{12} \lambda (1 + 3 \sin^2 \lambda)^{-1} \tag{4.4}$$

These coordinates have the property that lines of constant a are the lines of force for a dipole field.

The new canonical variables may be obtained from the generating function

$$F(z,\ \rho,\ p_a,\ p_b) = a(z,\ \rho)p_a + b(z,\ \rho)p_b \tag{4.5}$$

by employing the standard relations

$$p_z = \partial F/\partial z = (\partial a/\partial z)p_a + (\partial b/\partial z)p_b \tag{4.6a}$$

$$p_\rho = \partial F/\partial \rho = (\partial a/\partial \rho)p_a + (\partial b/\partial \rho)p_b \tag{4.6b}$$

$$a = \partial F/\partial p_a = a(z, \rho) \tag{4.7a}$$

$$b = \partial F/\partial p_b = b(z, \rho) \tag{4.7b}$$

By using the line element relations

$$\begin{aligned} ds^2 &= (h_a\, da)^2 + (h_b\, db)^2 \\ &= h_a{}^2[(\partial a/\partial z)\, dz + (\partial a/\partial \rho)\, d\rho]^2 + h_b{}^2[(\partial b/\partial z)\, dz + (\partial b/\partial \rho)\, d\rho]^2 \\ &= dz^2 + d\rho^2 \end{aligned} \tag{4.8}$$

one finds that

$$p_z{}^2 + p_\rho{}^2 = (p_a/h_a)^2 + (p_b/h_b)^2 \tag{4.9}$$

The Hamiltonian, equation 2.16, may now be written as

$$\mathcal{H} = \tfrac{1}{2}[(p_a/h_a)^2 + (p_b/h_b)^2] + V(a, b) \tag{4.10a}$$

$$V(a, b) = (2a^4 \cos^6 \lambda)^{-1}(a - 1)^2 \tag{4.10b}$$

In the new dipolar coordinates the rapid oscillation about the thalweg is described by the variables a and p_a, and the slower motion along the thalweg is described by b and p_b. This separation makes it possible to treat each degree of freedom individually. In effect, as far as the a,p_a motion is concerned, the behavior is analogous to that of a harmonic oscillator whose parameters (the quantities b and p_b) change slowly in time.

It is well known that in such circumstances the action integral associated with the oscillatory motion is an adiabatic invariant [*Born*, 1960]. One therefore expects that the quantity J defined by the equation

$$\begin{aligned} J(b, p_b) &= \oint p_a\, da \\ &= \oint h_a\left[2\mathcal{H} - 2V - \left(\frac{p_b}{h_b}\right)^2\right]^{1/2} da \end{aligned} \tag{4.11}$$

will be approximately constant throughout the course of an orbit. The integral is to be evaluated with b and p_b held fixed.

The simplest conclusion that can be drawn from the above discussion is that the canonical momentum p_b should assume (approximately) the same absolute value each time the particle crosses the equatorial plane, or

$$|p_b|\Big|_{b=0} = \text{constant} = \alpha \tag{4.12}$$

From the equation

$$\dot{b} = \partial\mathcal{H}/\partial p_b = p_b h_b{}^{-2} \tag{4.13}$$

and equations 4.1–4.4 the quantity α is given in the ρ-z variables by the relation

$$\alpha = \rho^3 \, |\dot{z}| \Big|_{z=0} \tag{4.14}$$

This result will be used extensively in the following section.

To extract more information, it is necessary actually to evaluate the integral 4.11. Unfortunately, this cannot be done in closed form, and we must be content with an expansion. Inspection of equations 2.18 and 4.10 shows that each of the quantities p_a^2,$(a-1)^2$, and p_b^2 are of order $(\gamma_1^4)^{-1}$. One may therefore consider making an expansion in $\epsilon = (\gamma_1^2)^{-1}$. It is often more convenient to treat each degree of freedom individually and write

$$p_a = O(\epsilon_1) \tag{4.15a}$$

$$p_b = O(\epsilon_2) \tag{4.15b}$$

We begin by expanding the integrand about the equilibrium point a_0. This point is defined to be that value of a about which oscillations occur in the limit of infinitesimally small oscillation, and it is therefore the solution of the relations

$$\partial p_a/\partial a = 0 \tag{4.16a}$$

$$p_a \to 0 \tag{4.16b}$$

where p_a is viewed as the function of a, b, p_b, obtained by solving equation 4.10a

$$p_a = h_a[2H - 2V - (p_b/h_b)^2]^{1/2} \tag{4.17}$$

Expansion of p_a in a power series about the point $a = 1$ and application of equations 4.16 gives

$$a_0 = 1 - \tfrac{1}{2} \cos^6 \lambda p_b^2 (\partial/\partial a)(1/h_b^2) + O(\epsilon_2^4) \tag{4.18}$$

where the quantities on the right are to be evaluated at $a = 1$.

At first sight, this result seems somewhat surprising since one might naively think that the thalweg $a = 1$ should be the point of equilibrium. However, after some elementary algebra, one finds that

$$(1/h_a h_b)(\partial/\partial a) h_b = 1/R \tag{4.19}$$

where R is the radius of curvature defined in section 3. With the use of this relation and equations 4.10, equation 4.18 may be rewritten in the implicit form

$$\nabla_\perp V(a_0) = v_\parallel^2/R \tag{4.20}$$

This expression shows that the equilibrium point is displaced from the thalweg by the centrifugal force caused by the particle's motion along the field line.

The terms in the integrand may now be expanded in the form

$$h_a = c_0 + c_1(a - a_0) + \cdots \tag{4.21}$$

$$[2H - 2V - (p_b/h_b)^2] = d_0 - d_2(a - a_0)^2 + d_3(a - a_0)^3 + \cdots \tag{4.22}$$

The coefficient d_1 vanishes because of the equilibrium conditions of equations

4.16. Substitution of these expansions into equation 4.11 gives

$$J(b, p_b) \simeq \oint da[c_0 + c_1(a - a_0)][d_0 - d_2(a - a_0)^2 + d_3(a - a_0)^3]^{1/2} \tag{4.23}$$

The integral can be most easily evaluated by the method of residues. The result is

$$J(b, p_b) = (\pi c_0 d_0/\sqrt{d_2}) + O(\epsilon_1^4) \tag{4.24}$$

or

$$J(b, p_b) \simeq (\pi/\omega)[2H - 2V - (p_b/h_b)^2] \tag{4.25}$$

where the quantities on the right-hand side are to be evaluated at the equilibrium value $a = a_0$.

How does the above result compare with that of Alfvén? Upon substituting equation 4.10*a* into equation 4.25, we find

$$J \simeq (\pi/\omega)[(p_a/h_a)^2 + 2V(a, b)] + (\pi/\omega)[(p_b/h_b)^2 - (p_b/h_b)^2\,|_{a=a_0} - 2V(a_0, b)] \tag{4.26}$$

By using the relation

$$v_\perp^2 = (p_a/h_a)^2 + 2V(a, b) \tag{4.27}$$

and equations 3.1, 4.10, and 4.19, this may be rewritten as

$$J = \pi(v_\perp^2/\omega) - (\pi/\omega)(v_\parallel^2/R)h_a(a - 1) + O(\epsilon^4) \tag{4.28}$$

or

$$M = J/2\pi + (1/2\omega)(v_\parallel^2/R)h_a(a - 1) + O(\epsilon^4) \tag{4.29}$$

Thus, in the canonical theory, M is no longer constant over an orbit. Instead, it depends on the instantaneous distance of the particle from the thalweg and, therefore, varies essentially with the cyclotron frequency.[2] In the limit of very low energy the variation of M is unimportant since, by equation 4.15, M is of order ϵ_1^2, whereas the variation in M is of order $\epsilon_1\epsilon_2^2$; and the Alfvén theory is recovered.

We close this section by giving a comparison of our approximate results, as expressed in equations 4.12, 4.14, and 4.29, with exact numerical solutions. Figures 8 through 11 show the values assumed by M and α on successive equatorial crossings plotted as a function of ρ. For ease of comparison, all curves have been normalized to unity at the thalweg $\rho = 1$. The results with several different initial conditions are shown, and the points are numbered in chronological order. As can be seen, the variation in M is approximately linear as predicted by equation 4.29. The quantity α is remarkably constant even for rather small γ_1. Consequently, the action integral J as defined by equation 4.11 must also be a very good adiabatic invariant. For example, in the extreme case of Figure 10, M changes drastically,

[2] Similar results for the general magnetic field have been obtained by *Kruskal*. See *Northrop* [1963*a*, p. 69]. Note that the 'ϵ' terminology used there is different than the convention adopted here. In our notation, the magnetic moment itself is of order ϵ^2.

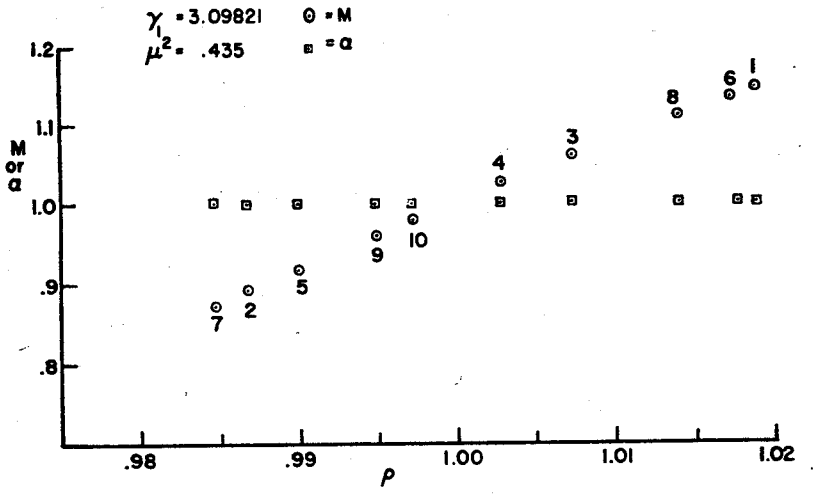

Fig. 8

Figs. 8–11. Values of M and α assumed on successive equatorial crossings as a function of ρ. Each orbit is labeled by its Störmer constant γ_1 and the value of μ^2 when $\rho = 1$. To facilitate easy comparison, the plotted values of M and α have been normalized by dividing them by their values at $\rho = 1$.

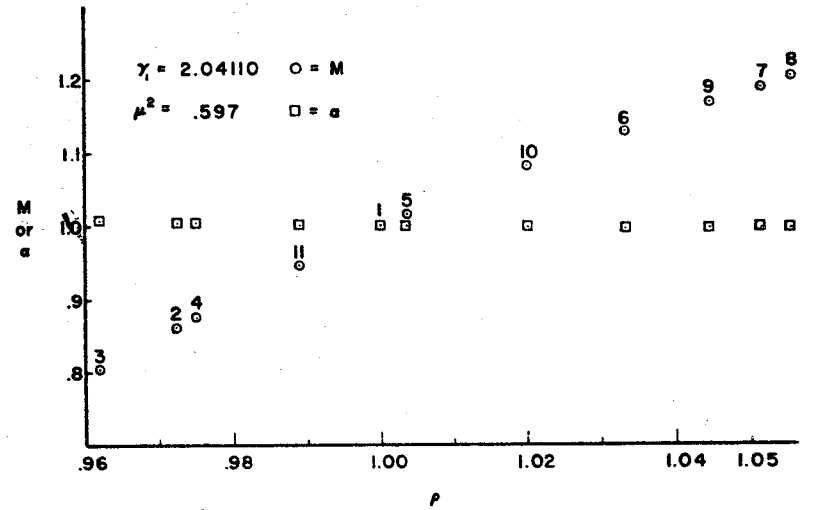

Fig. 9

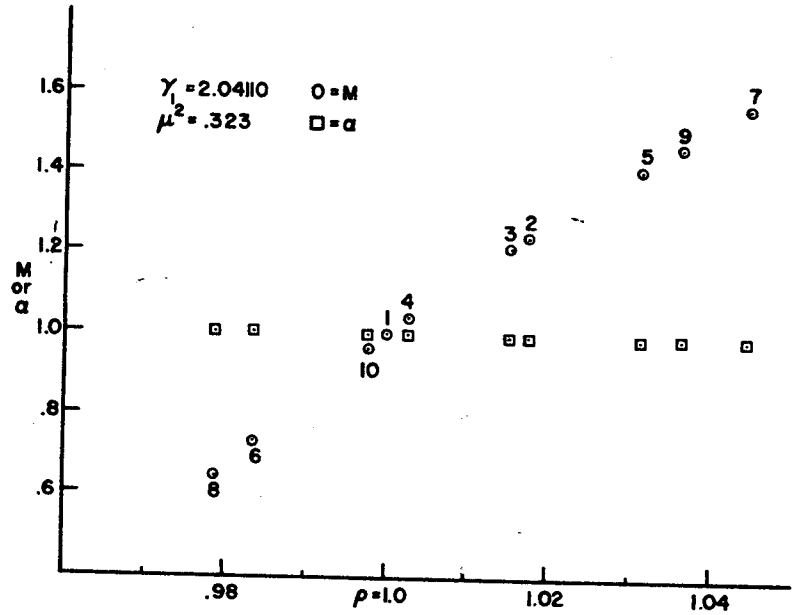
γ_1 = 2.04110 O = M
μ^2 = .323 □ = α
M or α
1.6
1.4
1.2
1.0
.8
.6
.98
ρ = 1.0
1.02
1.04

Fig. 10

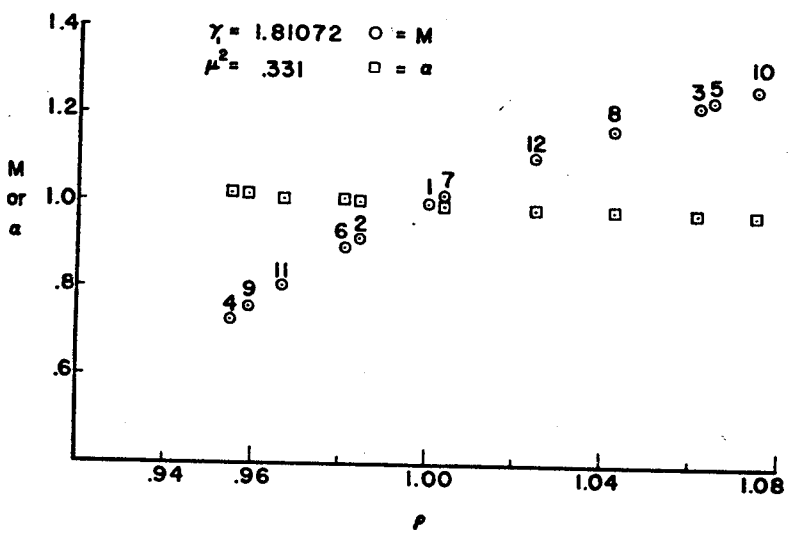
γ_1 = 1.81072 O = M
μ^2 = .331 □ = α
M or α
1.4
1.2
1.0
.8
.6
.94
.96
1.00
1.04
1.08
ρ

Fig. 11

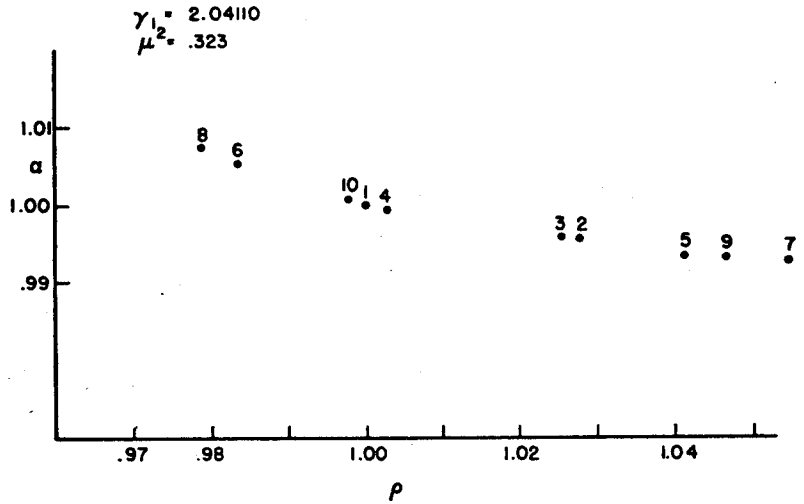

Fig. 12. A more detailed picture of the behavior of α for an extreme case.

$\Delta M/M \sim \pm 40\%$, whereas the corresponding change in α is relatively small, $\Delta\alpha/\alpha \sim \pm 1\%$. A more detailed plot of the behavior of α for this case is shown in Figure 12. These examples illustrate the superiority of the canonical perturbation theory over the conventional Alfvén theory at large energies.

The variation of α or M with ρ is not always monotonic or single-valued. There are instances where α and M are double-valued functions of ρ. Figures 13 and 14 illustrate a double-valued case. This kind of behavior occurs when the

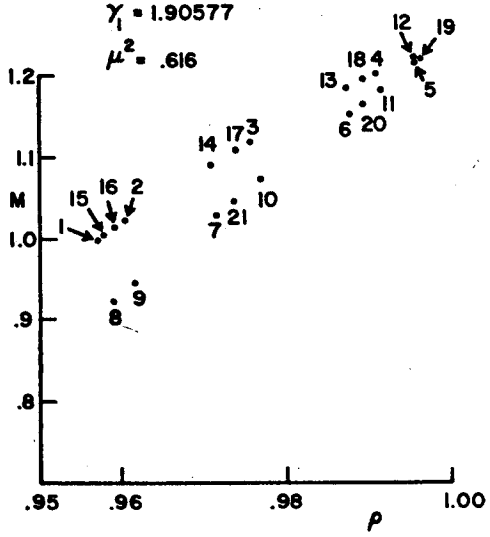

Fig. 13. An example in which M appears to be a double-valued function of p.

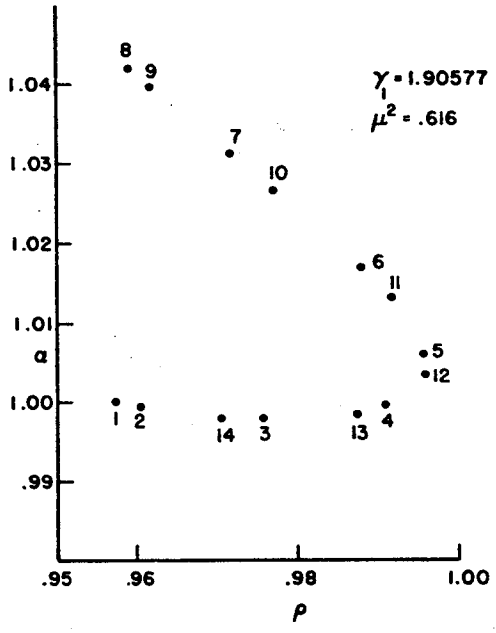

Fig. 14. The orbit of Figure 13 replotted to show the double-valued behavior of α.

initial conditions are near those for a periodic orbit. The particular case illustrated occurs near a periodic orbit having a rotation number R_a (defined in the next section) equal to 5. Figure 15 shows how the double-valued case goes over into

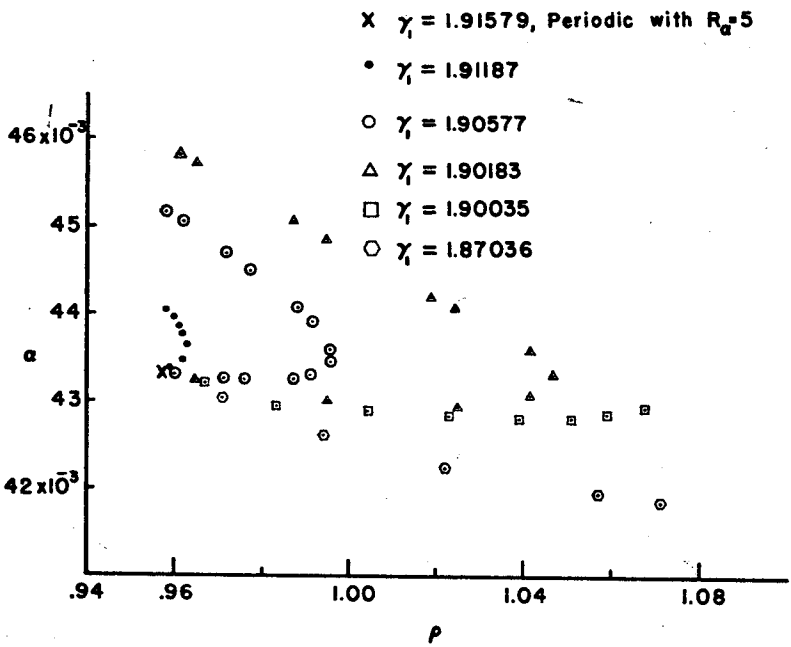

Fig. 15. The transition from double-valued to single-valued behavior with decreasing γ_1 near an orbit with $R_a = 5$. The quantity α is plotted in true scale.

the single-valued case as the initial conditions are changed. A similar phenomenon has been observed in numerical studies of orbits in a mirror machine [*Northrop*, 1963*a*, pp. 96–101]. This behavior cannot be explained by either the Alfvén or canonical perturbation theory; it awaits a more sophisticated approach.

5. APPLICATIONS

We now apply the results of the canonical theory to some instances in which the simple Alfvén theory is inadequate. We shall first discuss how the Alfvén theory can be extended to take into account, to first order, the variation in M given by equation 4.29. As a second application, we shall introduce the use of a Poincaré surface of section and employ canonical perturbation theory to calculate some of its features.

Extended Alfvén theory. To examine the effect of variations in M upon the Alfvén theory, it is useful to rewrite equation 4.28 in the form

$$v_\parallel = (v^2 - \omega J/\pi)^{1/2}(1 + f(a, b))^{-1/2} \tag{5.1a}$$

or

$$v_\parallel = v(1 - \omega J/\pi v^2)^{1/2}(1 - \tfrac{1}{2}f + (3/8)f^2 + \cdots) \tag{5.1b}$$

where

$$f(a, b) = (1/R)h_a(a - 1) + O(\epsilon^4) \tag{5.2}$$

This is the analog of equation 3.5 in the Alfvén theory, since in the dimensionless variables ω is given by

$$\omega = B/B_0 \tag{5.3}$$

We now consider the effect of the correction term f upon integrations based on the use of equation 5.1, for example, equations 3.11 and 3.19. When the correction term is included, the analog of equation 3.11 is

$$\int dt \left(1 - \frac{1}{2}f + \frac{3}{8}f^2 + \cdots\right) = \frac{1}{v}\int dl \left(1 - \frac{JB}{\pi v^2 B_0}\right)^{-1/2} \tag{5.4}$$

The only difference between equation 3.11 and equation 5.4 is the presence of the correction term f and the replacement of μ^2 by $J/\pi v^2$. We observe that f is small of order ϵ_1 and essentially oscillates in sign with the cyclotron frequency ω. Since f is oscillatory and ω is of order unity, the time integral of f over a bounce period must also be of order ϵ_1. By contrast, the bounce period itself is of order τ^{-1} and hence of order ϵ^{-1}. Thus, in comparison to the bounce period, the correction due to f is of order ϵ^2. It is therefore permissible, through order ϵ, to neglect the presence of f in the integration. We conclude that the first-order variation in M may be completely taken into account simply by redefining the quantity μ^2 of equation 3.10 in terms of J instead of M as was previously done

$$\mu^2 = J/\pi v^2 \tag{5.5}$$

The same conclusion holds for other integrations based on the use of equation 5.1.

It is also convenient to have an expression for μ^2 in terms of the quantity α defined in equations 4.12 and 4.14, since α is simply related to the initial conditions in the equatorial plane. For this purpose we use equations 4.21, 4.22, and 4.24. Examination of equations 4.1a and 4.3 shows that $\rho = a$ and $h_a = 1$ in the equatorial plane, so that in this case equations 4.22 and 4.24 may be rewritten as

$$\dot{\rho}^2 \,|_{z=0} = d_0 - d_2(a - a_0)^2 + d_3(a - a_0)^3 \tag{5.6}$$

$$J \,|_{z=0} \simeq \pi\, d_0/\sqrt{d_2} \tag{5.7}$$

Substitution of equation 4.14 into equation 2.16 and use of equation 2.22 gives a second expression for $\dot{\rho}^2$:

$$\dot{\rho}^2 \,|_{z=0} = W_0^2 - \alpha^2/\rho^6 - (1/\rho^4)(\rho - 1)^2 \tag{5.8}$$

Expansion of equation 5.8 in a power series about the equilibrium point a_0 given by equation 4.18 and comparison of the results with equation 5.6 now gives the desired relation

$$\mu^2 = \frac{1}{W_0^2}\frac{W_0^2 - \alpha^2 + 9\alpha^4 + \cdots}{(1 - 15\alpha^2 + \cdots)^{1/2}} \tag{5.9}$$

This definition of μ^2 is equivalent to that of equation 5.5 and replaces that of equation 3.10.

Poincaré surface of section. A Poincaré surface of section for a mechanical

system is defined to be a surface in phase-space which is crossed by every trajectory. Not every mechanical system possesses a surface of section; but in those cases in which a surface of section can be found, it serves as a useful tool for characterizing topological properties of orbits in the large [*Birkhoff*, 1927, p. 143]. On the basis of the Alfvén theory or the canonical perturbation theory, we intuitively expect that every orbit for the trapped Störmer problem when extended indefinitely backward and forward in time must cross the equatorial plane, so that in this case the three-dimensional surface given by $z = 0$ in the four-dimensional (ρ, z, p_ρ, p_z) phase-space must be a surface of section. This conjecture can be proved rigorously by a direct examination of the differential equations of motion [*De Vogelaere*, 1954]. In addition to crossing the surface of section, all orbits are constrained by energy conservation to lie on the three-dimensional surface given by equations 2.16–2.18. Therefore, the intersection of the surface of section with the surface of constant energy is two-dimensional, and the surface of section is effectively two-dimensional.

It is convenient to specify the location of a point on the surface of section by giving its value of ρ and $p_\rho = \dot{\rho}$. The value of $p_z = \dot{z}$ can then be found, up to a sign, from equations 2.16–2.18. The choice of sign is immaterial since the Hamiltonian (2.16) is even in z. With this convention, the surface of section may be taken to be the $\rho - \dot{\rho}$ plane.

To every point in the $\rho - \dot{\rho}$ plane consistent with energy conservation (the value of $\dot{z}^2$ calculated from equations 2.16–2.18 must be positive) there corresponds a definite trajectory in phase-space. Unless the trajectory so specified happens to be the one leading to the origin of the dipole, the trajectory will again intersect the equatorial plane, yielding another $\rho - \dot{\rho}$ point on the surface of the section. For the trajectory to the origin, the return path can be taken to be the same trajectory traced backward. Thus, under the action of the equations of motion, each point in the $\rho - \dot{\rho}$ plane is mapped into another point; and we obtain a transformation, T, of the $\rho - \dot{\rho}$ plane into itself.

A knowledge of T gives a great deal of information about the global properties of the trajectories themselves. For example, the problem of finding periodic trajectories is equivalent to the determination of those points in the $\rho - \dot{\rho}$ plane that are invariant under some integral power of T. This fact may be exploited to determine the initial conditions for certain classes of periodic orbits. An extensive discussion of the properties of T for the Störmer problem and its use in determining and classifying periodic orbits has been given by *De Vogelaere* [1958]. We note in passing that T is continuous and area-preserving.

A numerical exploration of the detailed properties of T requires a great deal of ingenuity and labor. It is therefore useful to have an approximate description of the properties of T. In what follows, we shall develop such a description on the basis of the canonical perturbation theory of section 4. Our theory will be approximate in nature and will become exact in the limit that $W_0^2 \to 0$ or $\gamma_1 \gg 1$.

According to the canonical theory, the quantity $\rho^3 |\dot{z}|$ may be expected to assume approximately the same value α each time the particle crosses the equatorial plane. Consequently, in this approximation the manifold M_α of points $(\rho, \dot{\rho})$ belonging to a given α must be invariant under T. By equation 5.8, the manifold may be written as

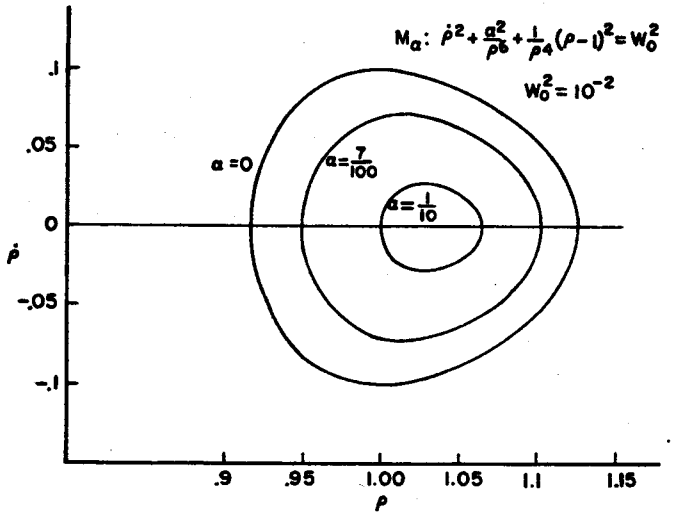

Fig. 16. The manifold M_α for three values of α.

$$M_\alpha : \dot\rho^2 + (\alpha^2/\rho^6) + (1/\rho^4)(\rho - 1)^2 = W_0^2 \tag{5.10}$$

Figure 16 shows a plot of the points in M_α for different values of α. For ease of graphing, W_0^2 has been chosen to be 10^{-2}. Examination reveals that the M_α are approximately a family of concentric circles. The circles decrease in size with increasing α until at $\alpha = \alpha_{max}$ they have degenerated into a point. The value of α_{max} may be found by increasing the value of α in equation 5.10 until the equation no longer has positive solutions for $\dot\rho^2$. The result is

$$\alpha^2_{max} = W_0^2 + 9W_0^4 + \cdots \tag{5.11}$$

Reference to equation 5.9 shows that when $\alpha = \alpha_{max}$, μ^2 vanishes. By equation 3.12 or Table 1, the vanishing of μ^2 corresponds to a mirror latitude λ_m of 90°. We therefore expect that the point given by M_α when $\alpha = \alpha_{max}$ corresponds to the initial conditions for a particle to go to the origin of the dipole. These initial conditions can be found by setting $\alpha = \alpha_{max}$ in equation 5.10 and solving for ρ and $\dot\rho$ with the result

$$\dot\rho = 0 \tag{5.12a}$$

$$\rho = 1 + 3W_0^2 + \cdots \tag{5.12b}$$

Comparing equations 5.12 with equation 2.47, we see that the canonical theory yields the same initial conditions as the first two terms of the asymptotic series (2.47).

It is also possible to use the canonical theory to solve approximately for the remaining points on the trajectory to the origin. By equation 5.5, the vanishing of μ^2 implies the vanishing of J. To the extent to which J is approximately constant, it must therefore vanish over the entire orbit. This can only occur if the particle moves in such a way that p_a is always zero and a is always at the equilibrium point a_0 given by equation 4.18. The trajectory through the origin is

thus approximately given by the equation

$$a = 1 + \cos^6 \lambda (p_b/h_b)^2 (1/h_b)(\partial/\partial a) h_b \tag{5.13}$$

Since p_a is zero and a is near the thalweg, the quantity $(p_b/h_b)^2 = v_\parallel^2$ is very nearly equal to W_0^2. The remaining parts of equation 5.13 can be simplified with the aid of equation 4.19 to give

$$a = 1 + W_0^2 \cos^6 \lambda (h_a/R) \tag{5.14}$$

Finally, the trajectory may be expressed in terms of the r and λ coordinates with the aid of equations 3.16, 4.1, and 4.3. The result is

$$r = \cos^2 \lambda + 3W_0^2 \cos^{10} \lambda (2 - \cos^2 \lambda)/(4 - 3 \cos^2 \lambda)^2 \tag{5.15}$$

Thus, the canonical theory correctly predicts the trajectory to the origin up to terms of order W_0^4. (This result has also been obtained by *Bossy* [1962].)

Thus far, we have seen that the manifold M_a of points in the $\rho - \dot{\rho}$ plane is approximately invariant under T. We now consider the action of T on M_a itself. Now M_a for a given a is approximately a circle. Therefore the effect of T is a rotation R_a sending each point in M_a to another point in M_a. Consider the particle motion as viewed in the $a - p_a$ plane. These are the variables that go over into $\rho - \dot{\rho}$ at the equator. Because the motion in the $a - p_a$ variables is approximately that of a harmonic oscillator (see section 4), the motion in the $a - p_a$ plane is essentially a rotation occurring with the cyclotron frequency ω. As a particle leaves the equator and returns after mirroring, the variables $\rho - \dot{\rho}$ go over to the variables $a - p_a$ and then reassume their original role. It is therefore convenient to define R_a as the number of rotations in the $a - p_a$ plane, i.e. the number of cyclotron gyrations made by the particle between equatorial crossings

$$R_a = \frac{1}{2\pi} \int \omega \, dt = \frac{1}{2\pi} \int \frac{\omega}{v_\parallel} \, dl \tag{5.16}$$

We now turn to the task of evaluating the integral for R_a. By equations 5.1 and 5.5, the integrand may be rewritten as

$$\omega = (v^2 - v_\parallel^2)/\mu^2 v^2 \tag{5.17}$$

Here we have omitted the correction term f, appearing in equation 5.1 in accordance with our discussion of the extended Alfvén theory. Equation 5.16 may now be rewritten in the form

$$R_a = \frac{1}{2\pi v \mu^2} \left[v \int \frac{dl}{v_\parallel} - \frac{1}{v} \int v_\parallel \, dl \right] = \frac{1}{2\pi v \mu^2} [2T(\mu) - I(\mu)] = \gamma_1^2 N(\mu) \tag{5.18}$$

The first integral is already familiar from equation 3.11. The second, $I(\mu)$, has been calculated by *McIlwain* [1961 and private communication] in connection with another problem. The functions $I(\mu)$ and $N(\mu)$ are given in Table 1. For ease of interpolation, the function $\mu^2 N(\mu)$ is also listed, since it exhibits considerably less variation than $N(\mu)$.

To summarize, the action of T on the $\rho - \dot{\rho}$ plane (within the approximations of the canonical theory) is to transform each point belonging to a given M_a into another point within the same M_a. The transformation within M_a is a rotation by R_a revolutions. The manifold M_a is given by equation 5.10 and the rotation number R_a can be found from equations 5.9 and 5.18 in conjunction with Table 1.

As a test of our conclusions about the action of T, we can again look at numerical solutions. We shall first compare the approximate theory and exact results for the rotation number R_a and then turn to a study of the manifold M_a.

For checking R_a, we will use a set of periodic orbits found numerically for $\gamma_1 = 1.81072$ by De Vogelaere [unpublished], who provided the initial conditions for these orbits. Figure 17 presents a comparison of the exact rotation number for

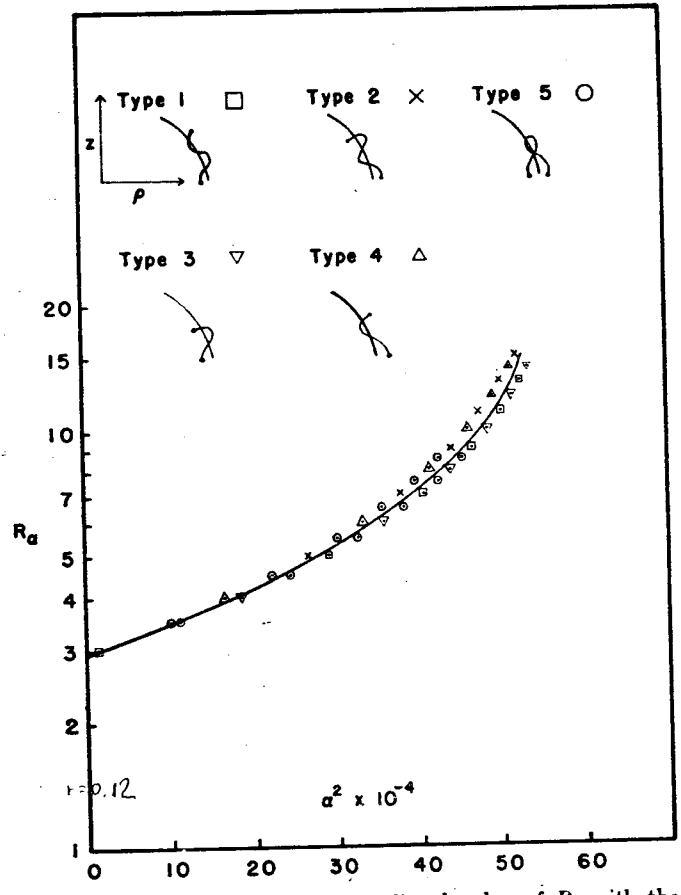

Fig. 17. A comparison of the predicted value of R_a with the actual value for several periodic orbits found numerically by De Vogelaere. The orbits are of five different types as illustrated at the top of the figure.

the periodic orbits and the approximate value of R_a obtained from equations 5.9 and 5.18 and Table 1. Five different types of orbits are shown. The trajectory in $\rho - z$ coordinates is illustrated for each type at the top of the figure. The orbits may be classified according to whether their rotation number is integral or half-integral. That is, the initial conditions in the $\rho - \dot{\rho}$ surface of section are invariant either under T or T^2. The orbits with integral R_a may be further classified by their point of departure from the equatorial plane and their mirror point. As can be seen, the predicted value of R_a falls between the actual value of R_a. It is interesting to note

that R_α depends on whether the launch point in the equatorial plane is on the inner side of the thalweg nearest the origin or on the outer side. It is quite insensitive, however, as to whether the mirror point is on the inner or outer side of the thalweg. The orbits with half-integral R_α cross the equatorial plane in two places with slightly different values of α^2, reflecting the fact that α is only approximately constant. These orbits appear to enjoy the properties of both inner and outer equatorial crossings.

We shall now explore to what extent the transformation T leaves M_α invariant. Figures 18 through 20 are $\rho - \dot{\rho}$ plots for the same orbits shown in Figures 8 through

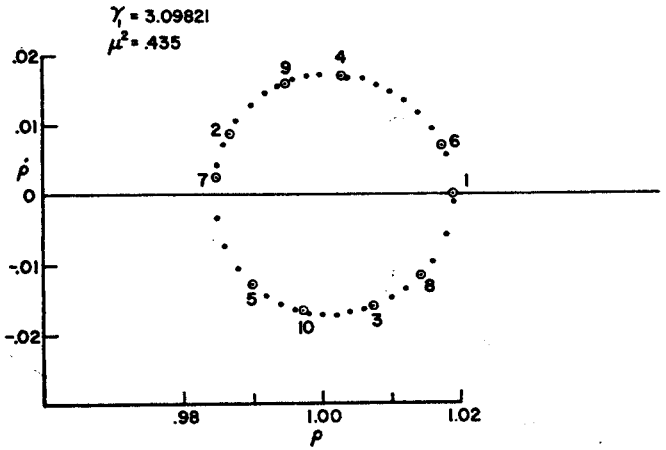

Fig. 18

Figs. 18–20. A comparison of M_α with series of successive points on the surface of section obtained by numerical integration. The manifold M_α is indicated by a set of open points.

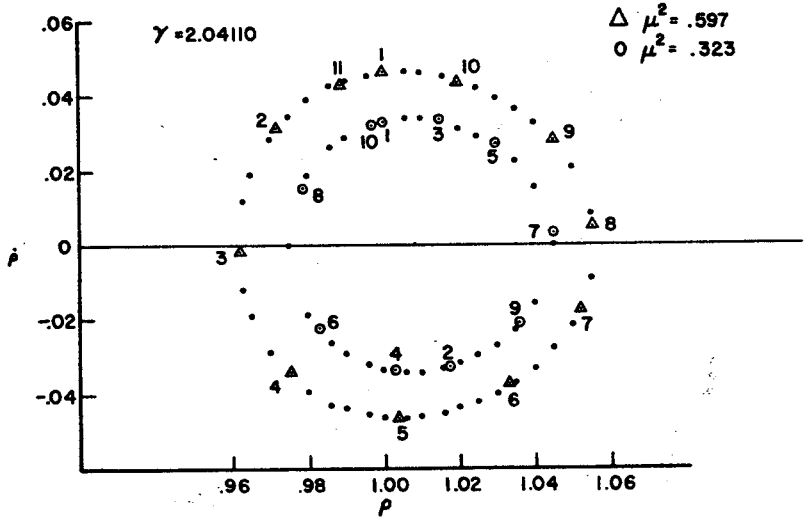

Fig. 19

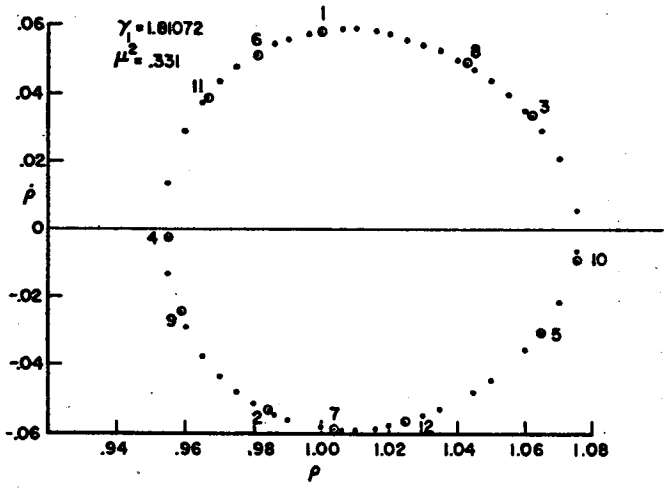

Fig. 20

11. For comparison, the manifold M_α given by equation 5.10 is also plotted as a set of open points. In general, the agreement is excellent and reflects the fact, already apparent from Figures 8 through 12, that α is remarkably constant. Figures 21 through 23 show selected orbits from Figure 15 replotted in $\rho - \dot{\rho}$ coordinates. The double-valued behavior is just barely discernible in Figures 21 and 22. It has the effect that the points tend to lie on a thin crescent as illustrated schematically at the top of Figure 21. In Figure 23, the vertices of the crescent have joined and the behavior is again single-valued.

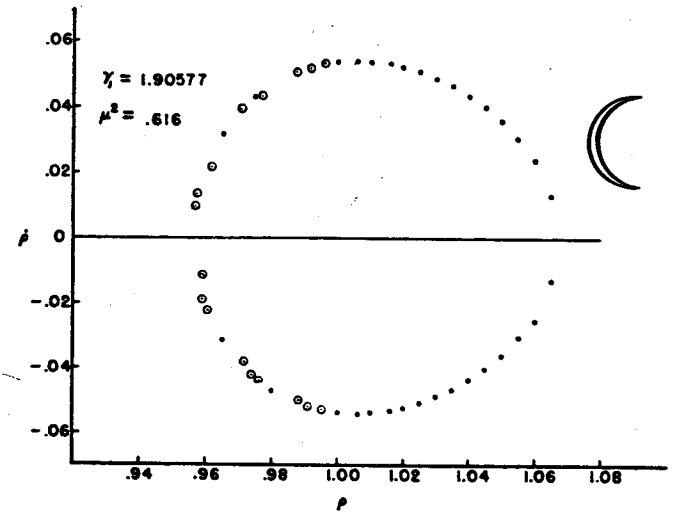

Fig. 21

Figs. 21–23. The transition from double-valued to single-valued behavior on the surface of section.

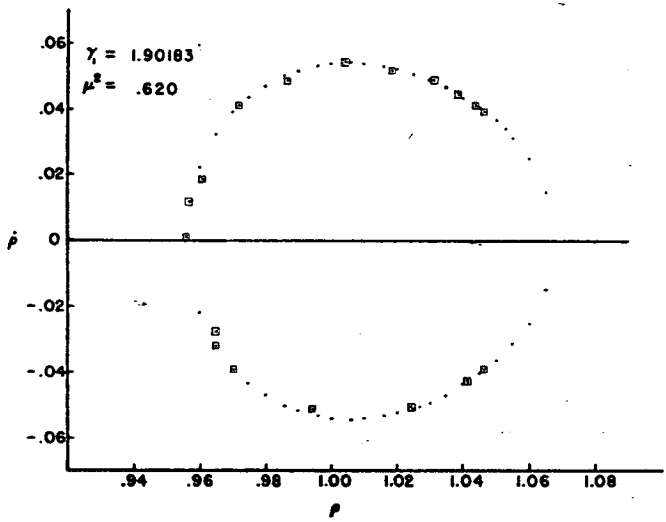

Fig. 22

6. THE LONG-TIME BEHAVIOR OF THE MAGNETIC MOMENT

All the approximate results of the previous sections are essentially based on the hypothesis that associated with the gyrating motion of a charged particle there is an approximately constant, or adiabatically invariant, quantity. In the Alfvén theory, this quantity is the magnetic moment given by equation 3.1. In the canonical perturbation theory, the magnetic moment is replaced by a more exact adiabatic invariant, the action variable of equation 4.28. In both theories, the role of the adiabatic invariant is that of a third constant of motion. This constant of motion, in conjunction with the first two given by the energy and the

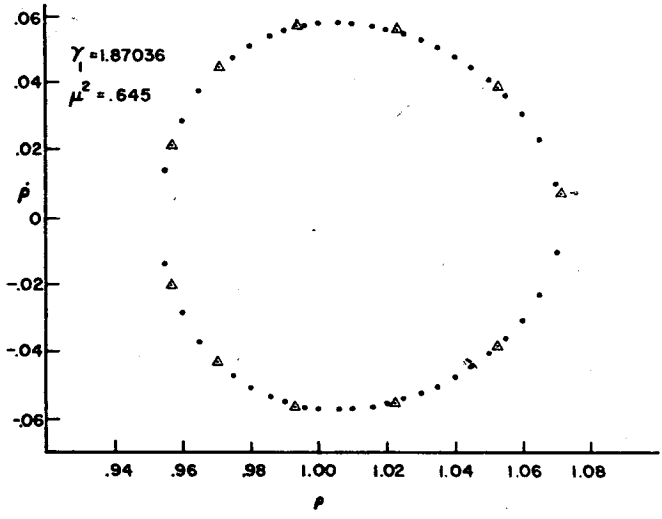

Fig. 23

canonical angular momentum (Equations 2.7 and 2.9), enables a complete (but approximate) solution of the equations of motion.

In this section, we shall explore in more detail the numerical behavior of the action variable J. This behavior is of special geophysical significance to the Van Allen radiation, as mentioned in section 3, since the value of J determines at what latitude a trapped particle will mirror. If a particle mirrors at too high a latitude, it will enter the earth's atmosphere and be lost from the trapped radiation.

The numerical results of the last section show that α and therefore J are remarkably constant from one equatorial crossing to the next. But this does not really answer the important question: what happens to J after many equatorial crossings? Does J change in such a way that it eventually becomes arbitrarily small, or does it remain in the neighborhood of some mean value, $\bar{J}$? Equivalently, do successive mirror points wander arbitrarily in latitude, or are they confined to the neighborhood of some mean latitude? If the mirror points do wander, how long does it take to go from one latitude to another? Clearly, the answer to such questions is crucial in determining the lifetime of the Van Allen radiation against atmospheric scattering.

Unfortunately, there is at present no known way of handling the problem analytically.[3] Straightforward numerical integration of the equations of motion is also useless with present-day computers, since the validity of the solution is vitiated by truncation and round-off errors long before one can compute the required number of reflections. For example, there are believed to be Van Allen protons whose lifetime against all loss mechanisms exceeds 10 years. During this time such particles undergo approximately 10^9 reflections.

Geophysics is not the only context in which this problem arises. It is also a matter of major concern in the design and construction of mirror machines for studies of controlled fusion. Surprisingly, workers in this field have found that, despite expectations to the contrary, long-term properties of orbits as observed experimentally appear to be predictable from the results of short-term numerical integration.

The method employed in the area of mirror machines is to make plots of the value assumed by M on successive equatorial crossings similar to those in Figures 8 through 11 (*Garren et al.* [1958]; *Northrop* [1963*a*, chapter 5]). If, upon close inspection, the points in a plot appear to fall on a smooth curve, the mirror points for this orbit are found experimentally to have long-term stability in a mirror machine. If, on the other hand, the numerical points are scattered, the experimentally observed orbit will have unstable mirror points. Moreover, the transition from 'smooth curve' to 'scattered' occurs quite suddenly as the initial orbit parameters are varied, so that there is a minimum of subjective uncertainty about to which category a given trajectory belongs.

We will now explore the consequences of assuming that a similar analysis

[3] See, however, the work of *Moser* [1962] and Gardner (unpublished) referred to by *Northrop* [1963*a*] which demonstrates the existence, under certain conditions, of curves similar to the M_a of section 5 that are rigorously invariant under the action of T. If such curves exist, all ρ-$\dot{\rho}$ points outside them must lead to stable orbits.

is valid for the Störmer problem. (An analysis of essentially this type has been independently performed by *Garmire* [1963] with results similar to those presented here.) Since α is more nearly constant than M, we have found it more convenient to make plots of α versus ρ similar to Figure 12. The use of α in place of M makes it possible to use a larger scale in plotting, thus permitting a closer inspection of the 'smoothness' of curves.

All the orbits presented so far, i.e., those in Figures 8 through 15, are of the smooth curve variety. Figures 24 through 31 show two families of orbits for

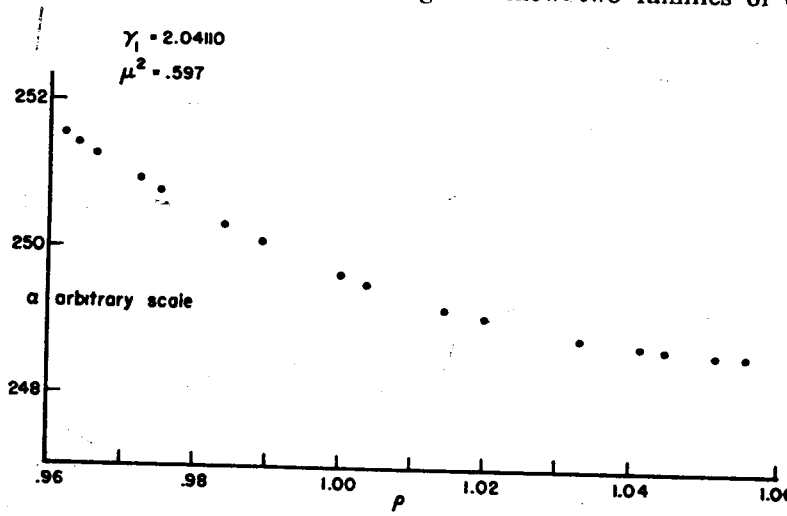

Fig. 24

Figs. 24–26. Smooth curve α-ρ plots for a given energy and increasing mirror latitudes. The α scale is arbitrary to facilitate plotting.

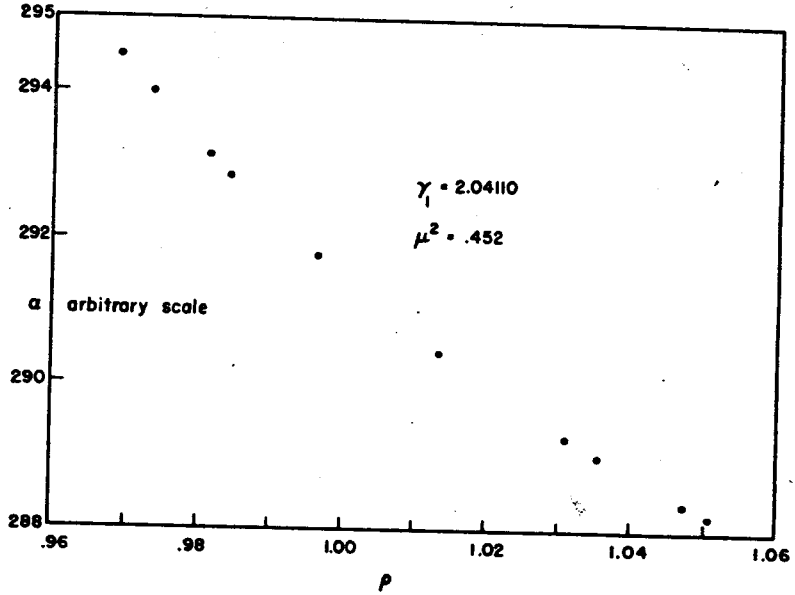

Fig. 25

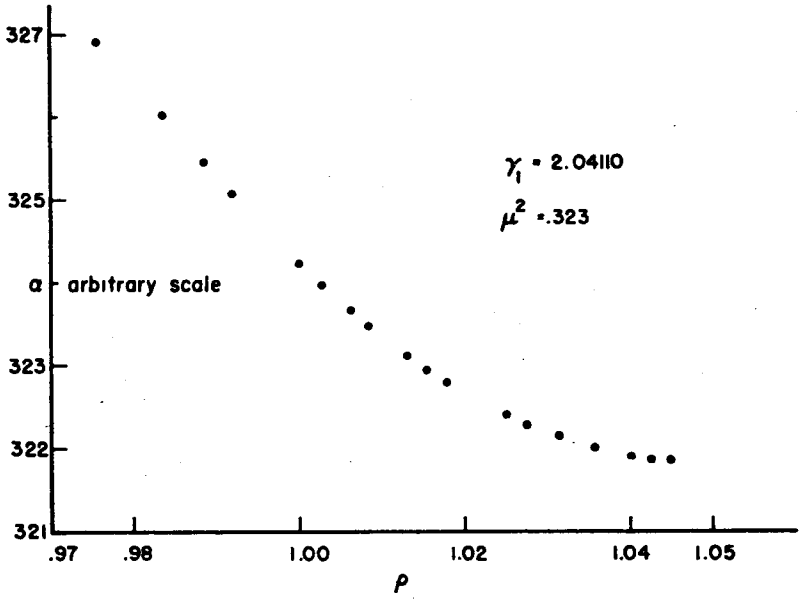

Fig. 26

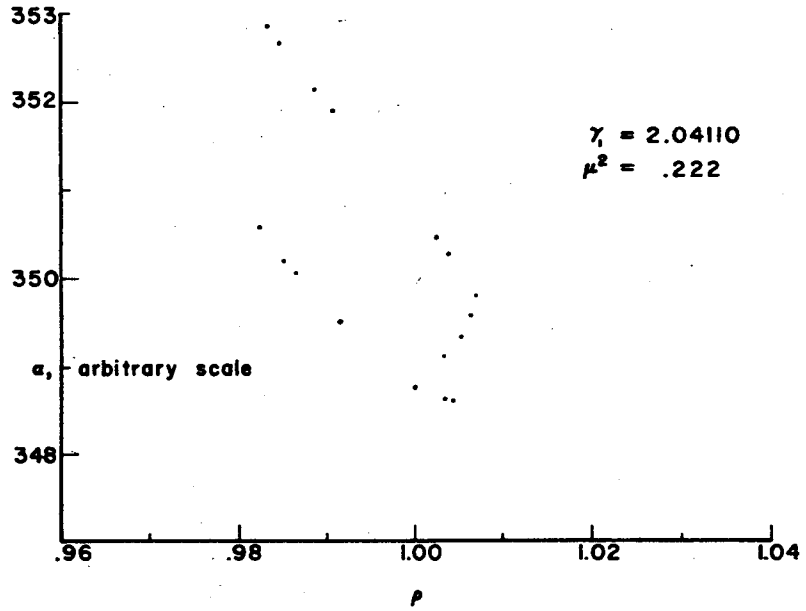

Fig. 27 A scattered α-ρ plot for the $\gamma_1 = 2.0411$ series illustrating the breakdown of the magnetic moment for trajectories with higher mirror latitudes.

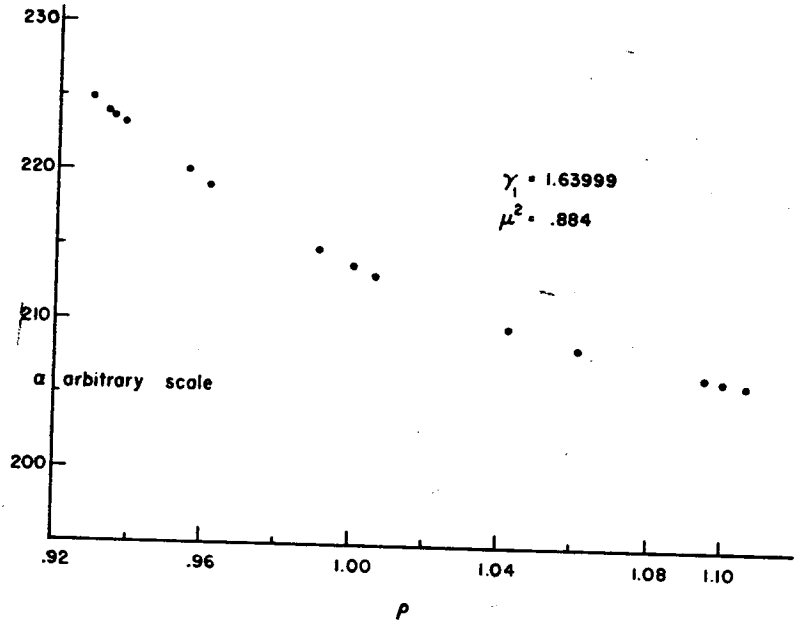

Fig. 28

Figs. 28–29. Smooth α-ρ plots for a smaller γ_1.

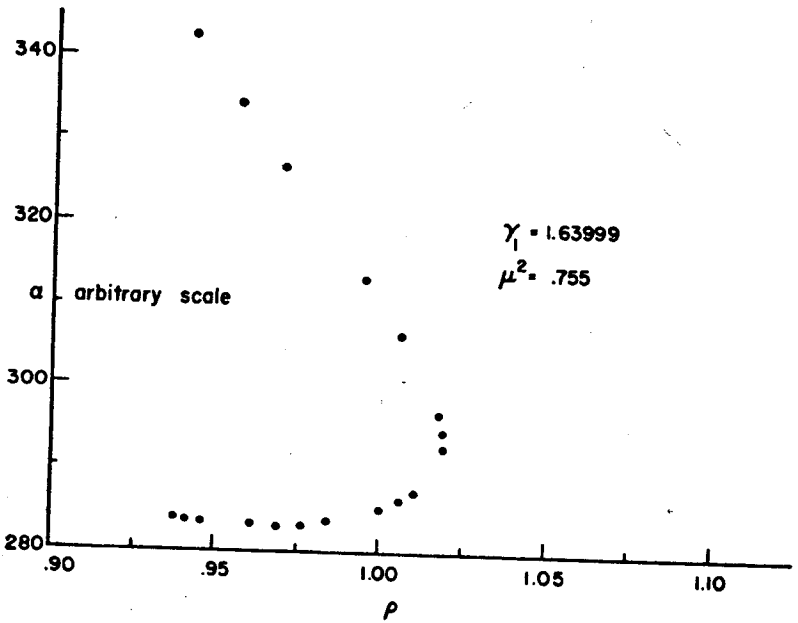

Fig. 29

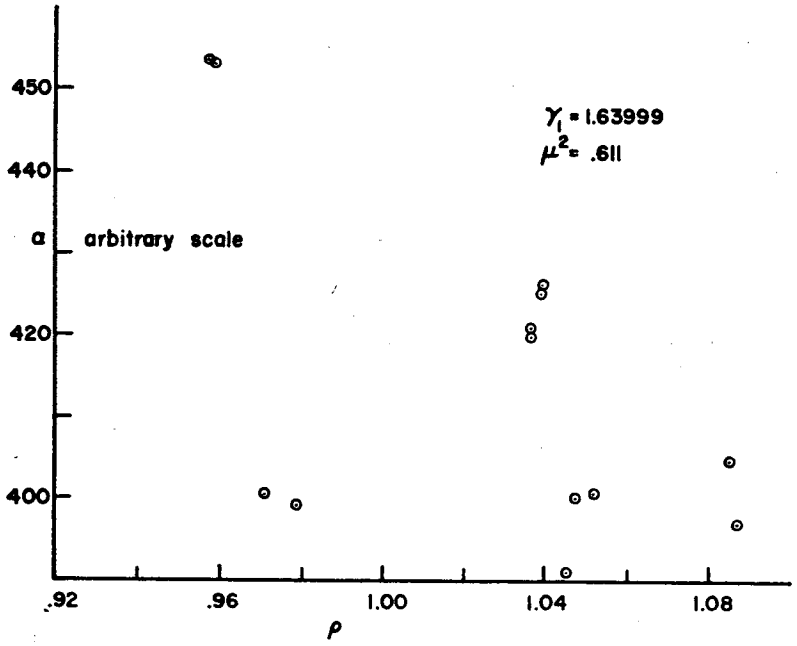

Fig. 30

Figs. 30–31. Scattered α-ρ plots for the $\gamma_1 = 1.63999$ series.

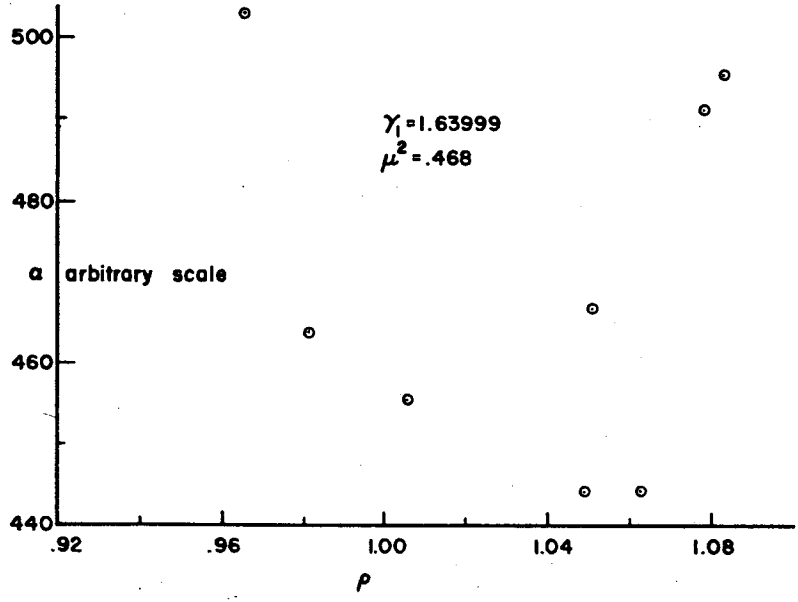

Fig. 31

$\gamma_1 = 2.04110$ and $\gamma_1 = 1.63999$, which contain curves of both the smooth and scattered type. The curves within each family differ by the value of μ^2 chosen for the initial conditions at the beginning of the numerical integration. The accuracy of the numerical solutions has been checked by reversing the sign of the particle velocity at the end of each integration run and then integrating back to the initial conditions. Evidently, for $\gamma_1 = 2.04110$, the trajectories having an initial μ^2 of 0.597, 0.452, and 0.323 are of the smooth variety. As μ^2 is further decreased, the $\alpha-\rho$ plot becomes scattered as illustrated in Figure 27 for $\mu^2 = 0.222$. For $\gamma_1 = 1.63999$, a similar transition takes place as the initial value of μ^2 is decreased. For $\mu^2 = 0.884$ and 0.755, Figures 28 and 29, the $\alpha-\rho$ plot is smooth. For smaller values of μ^2, Figures 30 and 31, the $\alpha-\rho$ plot is again scattered.

A graphical 'smooth curve' or 'scattered' analysis similar to that of Figures 24 through 31 has been performed for several other initial conditions. Figure 32

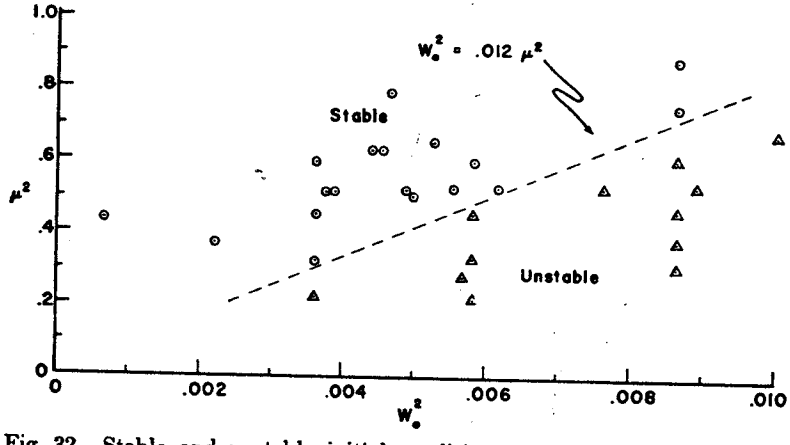

Fig. 32. Stable and unstable initial conditions as judged by the smooth or scattered criterion.

shows the result for each initial condition. Trajectories having a 'smooth curve' $\alpha-\rho$ plot are marked by a circle; trajectories with a 'scattered' plot are marked by a triangle.

It is evident from the figure that 'scattered' behavior sets in at larger values of μ^2 with increasing particle energy. If an orbit with a given energy and initial μ^2 is unstable in the sense that it yields a scattered $\alpha-\rho$ plot, we expect that orbits with a larger energy or smaller value of μ^2 will also be unstable. Conversely, if an orbit with a given energy and μ^2 is stable in the sense that it yields a smooth curve $\alpha-\rho$ plot, then those orbits with a smaller energy or larger μ^2 will also be stable. This consideration makes it possible to divide Figure 32 into regions of stability and instability. All initial conditions lying within the stable region should give trajectories with smooth $\alpha-\rho$ plots, and hence these trajectories should exhibit long-term trapping within a dipole field. Conversely, those orbits whose initial conditions lie within the unstable region should have scattered $\alpha-\rho$ plots and are not expected to exhibit long-term trapping.

The above discussion provides a criterion for long-term containment in a magnetic dipole field similar to that used for mirror machines. We now enquire to what extent the Van Allen radiation satisfies this criterion. The Van Allen radiation has been shown to consist of two components: (1) a hard proton component, the proton belt, centered at about 10^4 km from the earth's magnetic axis, and (2) an electron component that extends through the region occupied by the proton belt and is terminated at its outer boundary by the interface between the earth's magnetic field and the low energy plasma streaming from the sun. (See, for example, *Fan et al.* [1960], *Freden and White* [1959, 1960], *Holly and Johnson* [1960], *Vernov et al.* [1959], *Walt et al.* [1960].) The approximate extent of each component is shown in Figure 33, which presents contours of constant flux in space [*Dessler*, 1961].

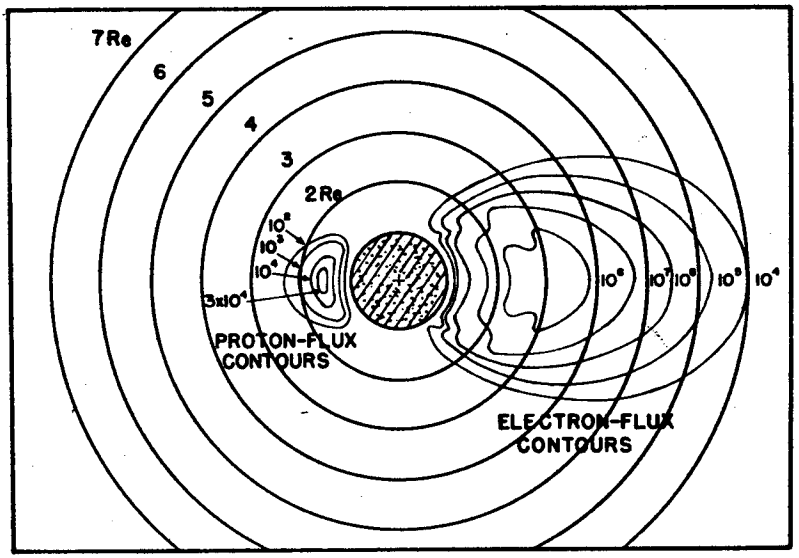

Fig. 33. Contours of constant flux in the Van Allen radiation. (Courtesy of Stanford University Press.)

One of the most striking features of the Van Allen radiation is that the hard proton component of the radiation essentially terminates at about 2 R_E from the earth's center. If it is assumed that the extent of the proton belt is governed by the breakdown of the adiabatically invariant action integral [*Singer*, 1959], the shape of the populated regions in space for various energies can be calculated from Figure 32 with the aid of Figures 2 and 4 and Table 1. To within sufficient accuracy, the boundary between the regions of stability and instability in Figure 32 can be represented by the expression

$$W_0^2 = 0.012\mu^2 \tag{6.1}$$

If anything, this formula underestimates the region of stability for μ^2 near unity, since in this case we are dealing with nearly equatorial orbits. As discussed in section 2, these orbits are stable in the Poincare sense provided $\gamma_1 > 1.3137$ or

$W_0^2 < 2.0984 \times 10^{-2}$. Choosing a definite energy and field line, one obtains the equivalent value of γ_1 and W_0^2 from Figures 2 and 4. Alternatively, one may also use equations 2.14, 2.20, and 2.22. Using equation 6.1, we obtain the minimum value of μ^2 consistent with stability. This minimum value of μ^2 is converted into a maximum mirror latitude by using Table 1. Thus we find that a given field line can be populated by protons of a definite energy over a range of latitude up to a certain maximum latitude. Figure 34 shows two maximum energy contours so obtained.

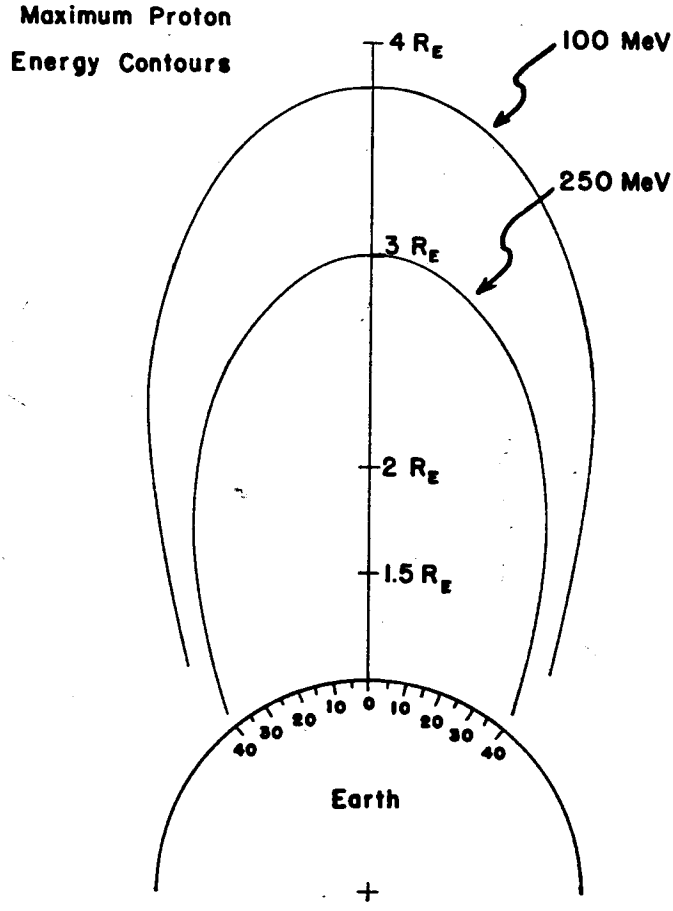

Fig. 34. Two maximum energy contours calculated on the basis of the breakdown of the magnetic moment using equation 6.1.

A similar analysis may be made for electrons. Reference to Figure 3 shows that owing to the smaller electron mass electron orbits are characterized by much larger values of γ_1 and are therefore stable except in regions very far from earth. At far distances, the earth's field is severely distorted by the solar plasma so that an analysis of orbits in terms of a dipole field is meaningless.

How does the shape of the actual proton belt compare with the hypothetical

model? The answer depends on where we look. At high latitudes, the model agrees with experiment fairly well. For example, *Imhof and Smith* [1964] find that protons on the field line with $r_0 = 1.9\ R_e$ and mirroring with $\lambda_m \geq 27°$ have a maximum energy of ~200 Mev. Using Table 1, equation 6.1, and Figures 2 and 4, we find that the maximum energy permitted by the breakdown of the magnetic moment is ~400 Mev. The discrepancy of a factor of 2 can perhaps be attributed to the departure of the earth's field from that of a pure magnetic dipole [*Garmire*, 1963].

For orbits that remain near the equatorial plane, the discrepancy is much larger. Figure 35 shows contours of constant flux near the equatorial plane for

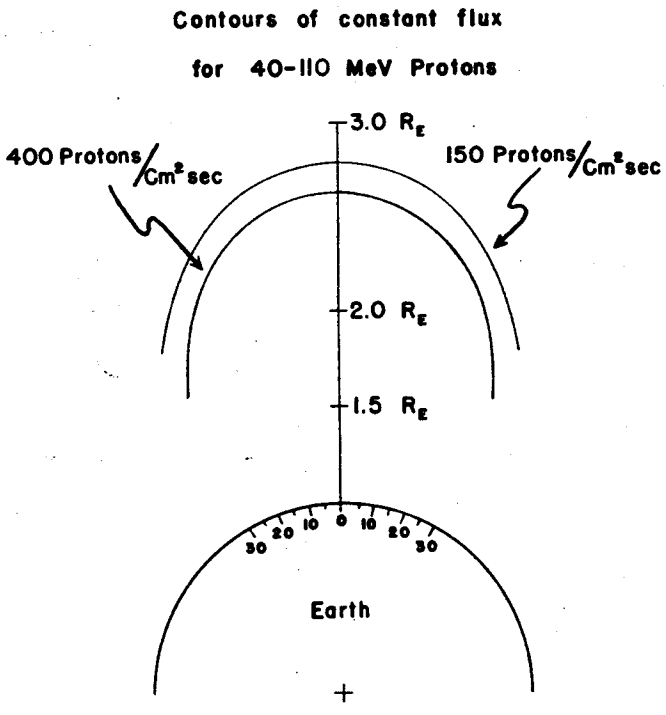

Fig. 35. Contours of constant proton flux as measured by Explorer 15.

40- to 110-Mev protons as measured by Explorer 15 [*McIlwain*, 1963]. It is apparent that there are large regions of space that, on the basis of a static dipole field, are capable of containing energetic protons and yet do not. There is no reason to doubt that energetic protons are injected into this region. According to current theory a substantial part of the proton belt arises from cosmic-ray albedo neutron decay. On the basis of this theory, almost as many protons should be deposited at 2 R_e from the earth's center as are deposited near the earth's surface. Hence, there is ample reason to believe that energetic protons are injected in sufficient amounts into the unpopulated regions to produce substantial trapped radiation [*Singer and Lenchek*, 1962].

There are at least two possible explanations for the discrepancy: (1) the higher multipole moments in the earth's magnetic field may again play an important role in determining an orbit's stability or (2) the protons at the outer edge of the inner belt may be affected by short-term dynamic fluctuations in the earth's field, for example, hydromagnetic waves [*Wentzel*, 1961; *Dragt*, 1961]. As mentioned earlier, the first explanation may play a role in determining the shape of the proton belt at high latitudes; however, there are two reasons for believing that this explanation cannot have a large effect on those orbits that mirror near the equator. The first reason is that the introduction of substantial azimuthal gradients in the magnetic field of experimental mirror machines appears to have little effect on the stability of orbits [*Gibson et al.*, 1963]. The second reason is that at large distances from the earth the higher multipoles in the earth's field become less important compared to the dipole term. For example, at a distance of 2 R_e from the earth's center, the magnetic field due to the quadrupole term in the earth's field is only about 4% of that due to the dipole term [*Chapman and Bartels*, 1941]. We therefore conclude that other effects in addition to the breakdown of the magnetic moment must play a large role in determining the outer boundary of the proton belt.

Acknowledgments. The major part of this work was performed at the University of Maryland during the year 1962–1963. I am indebted to Mr. W. E. Francis, who performed much of the numerical work using IBM 7090 time provided by the Lockheed Missiles and Space Company. I thank Professor J. R. Oppenheimer for his kind hospitality at the Institute for Advanced Study.

APPENDIX

In this appendix the numerical method employed in integrating the equations of motion is described. We shall first derive some integration formulas for polynomials and then turn to the equations of motion.

Let $y(t)$ be an arbitrary polynomial in t and let h be a small time increment. We use the notation

$$y_n = y(nh) \tag{A1}$$

and define a backwards difference operator ∇ by the equation

$$\nabla y_n = y_n - y_{n-1} \tag{A2}$$

From Taylor's theorem it follows that

$$\nabla y_n = (1 - e^{-hD})y_n \tag{A3}$$

where D is the differentiation operator

$$D = d/dt \tag{A4}$$

Since equation A3 is true for arbitrary polynomials, we obtain a symbolic relation between D and ∇

$$D = -h^{-1} \log (1 - \nabla) \tag{A5}$$

Let f denote the second time derivative of y

$$D^2 y_n = f_n \tag{A6}$$

It then follows that

$$\nabla^2 y_n = \nabla^2 D^{-2} f_n \tag{A7}$$

where the factor ∇^2 is inserted to annihilate the arbitrary linear function of t resulting from the use of the improper inverse operator D^{-2}. Substitution of equation A5 into equation A7 now gives an integration formula for y in terms of its second derivative

$$\begin{aligned}\nabla^2 y_n &= h^2 \nabla^2 [\log (1 - \nabla)]^{-2} f_n \\ &= h^2(1 - \nabla + 1/12\nabla^2 + 0\nabla^3 - 1/240\nabla^4 - 1/240\nabla^5 + \cdots) f_n \end{aligned} \tag{A8}$$

A similar formula relating y_n to f_{n-1} may be obtained by multiplying both sides of equation A8 by $(1 - \nabla)^{-1}$.

$$\nabla^2 y_n = h^2(1 + 0\nabla + 1/12\nabla^2 + 1/12\nabla^3 + 19/240\nabla^4 + 3/40\nabla^5 + \cdots) f_{n-1} \tag{A9}$$

Equations A8, A9 are true for arbitrary polynomials. We now assume that y contains no powers in excess of the sixth. The power series in ∇ may then be truncated beyond terms of order ∇^4. After truncation and expansion of the powers of ∇ by the definition of equation A2, equations A8 and A9 become

$$y_n - 2y_{n-1} + y_{n-2} = h^2/240(19f_n + 204f_{n-1} + 14f_{n-2} + 4f_{n-3} - f_{n-4}) \tag{A10}$$

$$y_n - 2y_{n-1} + y_{n-2} = h^2/240(299f_{n-1} - 176f_{n-2} + 194f_{n-3} - 96f_{n-4} + 19f_{n-5}) \tag{A11}$$

Equations A10, A11 are essentially the results that we will need. They are still in a somewhat inconvenient form since the left-hand sides are second differences. This defect may be remedied by summing each equation over n from $n = 4$ to $n = n_0 + 1$. The result is

$$y_{n+1} = y_n + (h/240)(19g_{n+1} + 204g_n + 14g_{n-1} + 4g_{n-2} - g_{n-3}) \qquad n \geq 3 \tag{A12}$$

$$y_{n+1} = y_n + (h/240)(299g_n - 176g_{n-1} + 194g_{n-2} - 96g_{n-3} + 19g_{n-4}) \quad n \geq 3 \tag{A13}$$

where g_n is defined by the relations

$$g_n = g_{n-1} + hf_n \qquad n \geq 0 \tag{A14}$$

$$g_{-1} = (1/h)[y_3 - y_2 - (h^2/240)(19f_3 + 223f_2 + 237f_1 + 241f_0)] \tag{A15}$$

and the index n_0 is again replaced by n.

We now describe the integration procedure and how it is applied, for example, to the equations of motion in ξ, η coordinates. When written in second-order form, the equations of motion read

$$\xi'' = -\tfrac{1}{2}\,\partial U/\partial \xi = F^1(\xi, \eta) \tag{A16}$$

$$\eta'' = -\tfrac{1}{2}\,\partial U/\partial \eta = F^2(\xi, \eta) \tag{A17}$$

By letting Y and F be two-component vectors having the entries (ξ, η) and (F^1, F^2), respectively, the pair of equations can be written more compactly as

$$Y'' = F(Y) \tag{A18}$$

Assume for the moment that the value of Y is known for $t = 0, h, 2h, 3h$. That is,

we know the values Y_0 to Y_3. From these values compute F_0 to F_3 where F_n is defined by

$$F_n = F(Y_n) \tag{A19}$$

Then the value of Y_4 can be predicted from equations A13, A14, and A15 by setting $n = 3$ and reinterpreting the quantities y, f, and g as vectors, Y, F, and G. We now solve equation A12 for a more accurate, or corrected, value of Y_4 by iteration, using the predicted value of Y_4 as a first iterate. The iteration process is terminated when successive iterates differ by less than some preassigned error.

From Taylor's theorem and differentiability conditions, which are obviously met, it follows that Y may be represented as a sixth order polynomial in t with an error of order h^7. We thus expect that the value of Y_4 obtained from equation A12 will be correct to this order. A more careful analysis shows that the error is given by $-(1/240)h^7Y^{VII}(\lambda)$ where $4h \leq \lambda \leq 0$. The whole process may now be repeated using the quantities Y_1 to Y_4 as initial values to compute Y_5, etc., and we thus obtain a numerical solution of the equations of motion.

It still remains to be explained how the starting values Y_1 to Y_3 are obtained from the initial conditions Y_0 and Y_0'. They may be calculated either by a Taylor expansion and the equations of motion or by numerical integration employing a Runge-Kutta [*Hildebrand*, 1956] method which is self starting and therefore requires no knowledge of the values of Y previous to Y_0.

It is worth remarking that before using the 'summed predictor corrector method' described above, we tried several of the common self starting integration schemes, plain and modified Euler and Runge-Kutta, for integrating the whole trajectory. They were all found to give too much cumulative error for long integration runs.

REFERENCES

Alfvén, H., *Cosmical Electrodynamics*, pp. 13–36, Oxford at the Clarendon Press, 1950.

Alfvén, H., and C. Falthammar, *Cosmical Electrodynamics*, pp. 18–70, Oxford at the Clarendon Press, 1963.

Avrett, E. H., Particle motion in the equatorial plane of a dipole magnetic field, *J. Geophys. Res., 67*, 53, 1962.

Birkhoff, G. D., *Dynamical Systems*, American Mathematics Society, New York, 1927.

Born, M., *The Mechanics of the Atom* (English translation by J. W. Fisher), p. 54, Frederick Ungar Publishing Company, New York, 1960.

Bossy, L., Le probleme de Störmer et le mouvement des particules dans les ceintures de radiation, *Ann. Geophys., 18*, 198–220, 1962.

Chapman, S., and J. Bartels, *Geomagnetism*, Vol. 2, Chap. 28, Oxford at the Clarendon Press, 1941.

Dessler, A. J., Penetrating Radiation, *Satellite Environment Handbook*, edited by F. S. Johnson, pp. 49–69, Stanford University Press, Stanford, California, 1961.

De Vogelaere, R., L'Equation de Hill et le problème de Störmer, *Can. J. Math., 2*, 440, 1950.

De Vogelaere, R., Surface de section dans le probleme de Störmer, *Acad. Roy. Belg. Bulletin Classe des Sciences, 40*, 705, 1954.

De Vogelaere, R., On the structure of symmetric periodic solutions of conservative systems, with applications, *Contributions to the Theory of Nonlinear Oscillations*, vol. 4, edited by S. Lefschetz, p. 53, Princeton University Press, Princeton, N. J., 1958.

Dragt, A. J., Effect of hydromagnetic waves on the lifetime of Van Allen radiation protons, *J. Geophys. Res., 66*, 1641, 1961.

Eisenhart, L. P., *Differential Geometry*, p. 150, Princeton University Press, Princeton, New Jersey, 1947.

Fan, C. Y., P. Meyer, and J. A. Simpson, Trapped and cosmic radiation measurements from Explorer VI, *Space Research, First International Space Science Symposium*, edited by H. K. Kallman-Bijl, pp. 951–966, North Holland Publishing Company, Amsterdam, 1960.

Freden, S. C., and R. S. White, Protons in the earth's magnetic field, *Phys. Rev. Letters, 3*, 9–11, 1959.

Freden, S. C., and R. S. White, Particle fluxes in the inner radiation belt, *J. Geophys. Res., 65*, 1377–1383, 1960.

Gall, R., Motion of charged particles in slowly varying fields to the first order of approximation, *J. Geophys. Res. 68*, 3565–3576, 1963.

Garmire, G., Geomagnetically trapped protons with energies greater than 350 Mev, *J. Geophys. Res., 68*, 2627–2638, 1963.

Garren, A., R. J. Riddell, L. Smith, G. Bing, L. R. Henrich, T. G. Northrop, and J. E. Roberts, *Proc. Second U. N. International Conf. on Peaceful Uses of Atomic Energy, Theoretical and Experimental Aspects of Controlled Nuclear Fusion* p. 65, United Nations, Geneva, Switzerland, 1958.

Gibson, G., W. C. Jordan, and E. J. Lauer, Particle behavior in a static, asymmetric, magnetic mirror geometry, *Phys. Fluids, 6*, 133–141, 1963.

Graef, C., and S. Kusaka, On periodic orbits in the equatorial plane of a magnetic dipole, *J. Math. Phys., 17*, 43, 1938.

Hamlin, D. A., R. Karplus, R. C. Vik, and K. M. Watson, Mirror and azimuthal drift frequencies for geomagnetically trapped particles, *J. Geophys. Res., 66*, 1, 1961.

Hayakawa, S., and H. Obayashi, An effect of nonadiabacity on the structure of radiation belts, *J. Geophys. Res., 68*, 3311–3313, 1963.

Hildebrand, F. B., *Introduction to Numerical Analysis*, p. 233, McGraw-Hill Book Company, New York, 1956.

Holly, F. E., and R. G. Johnson, Measurement of radiation in the lower Van Allen belt, *J. Geophys. Res., 65*, 771–772, 1960.

Hones, E. W., Jr., Motion of charged particles trapped in the earth's magnetosphere, *J. Geophys. Res., 68*, 1209, 1963.

Imhof, W. L., and R. V. Smith, Proton intensities and energy spectrums in the inner Van Allen Belt, *J. Geophys. Res., 69*, 91–100, 1964.

Lemaitre, G., and L. Bossy, Sur un cas limite du probleme de Störmer, *Acad. Roy. Belg. Bulletin Classe des Sciences, 31*, 357–364, 1945.

Malmquist, J., Sur les systemes d' equations differentielles, *Ark. Math. Astr. och Fysik 30 A, 5*, 1–8, 1944.

McIlwain, C. E., Coordinates for mapping the distribution of magnetically trapped particles, *J. Geophys. Res., 66*, 3681, 1961.

McIlwain, C. E., The radiation belts, natural and artificial, *Science, 142*, 355–361, 1963.

Moser, J., On invariant curves of area-preserving mappings of an annulus, *Nachr. Akad. Wiss. Goettingen, II Math.-Physik. Kl.*, 1, 1962. P גמ 701 1962

Northrop, T. G., *The Adiabatic Motion of Charged Particles*, Interscience Publishers (John Wiley & Sons), New York, 1963*a*.

Northrop, T. G., Adiabatic charged particle motion, *Rev. Geophys., 1*, 283–304, 1963*b*.

Ray, E. C., On the motion of charged particles in the geomagnetic field, *Ann. Phys. N. Y., 24*, 1–18, 1963.

Singer, S. F., Cause of the minimum in the earth's radiation belt, *Phys. Rev. Letters, 3*, 188–190, 1959.

Singer, S. F., and A. M. Lenchek, *Prog. in Elementary Particle and Cosmic Ray Physics*, V4, Chapter 3, 1962.

Störmer, C., Sur les trajectories des corpuscles electrises dans l'espace sous l'action du magnetisme terrestre avec application aux aurores boreales. *Arch. Sci. Phys. Nat., 24*, 1907.

Störmer, C., Resultats des calculs numeriques des trajectoires des corpuscles electriques dans

le champ d'un aimant elementaire, *Videnskabs-Selskabets Skrifter (Norske Videnskaps-Akademi i Oslo) Math-naturv. Klasse 4*, 1, 1913.

Störmer, C., *The Polar Aurora*, Oxford at the Clarendon Press, Oxford, 1955.

Van Allen, J. A., G. H. Ludwig, E. C. Ray, and C. E. McIlwain, *Jet Propulsion, 28*, 588 1958.

Vernov, S. N., A. E. Chudakov, P. V. Vakulov, and Yu. I. Logachev, Study of terrestria corpuscular radiation and cosmic rays during the flight of a cosmic rocket, *Soviet Phys "Doklady," 4*, 338–342, 1959.

Walt, M., L. F. Chase, Jr., J. Cladis, W. L. Imhof, and D. J. Knecht, Energy Spectra and Altitude Dependence of Electrons Trapped in the Earth's Magnetic Field, *Space Research First International Space Science Symposium*, pp. 910–920, edited by H. K. Kallman-Bijl, North Holland Publishing Co., Amsterdam, 1960.

Wentzel, D. G., Hydromagnetic waves and the trapped radiation, *J. Geophys. Res., 66*, 359–363 1961.

Whittaker, E. T., and G. N. Watson, *Modern Analysis*, p. 406, Cambridge University Press London, 1958.

(Manuscript received September 9, 1964.)